

EFFECT OF FILM DEPOSITION CONDITIONS ON THE  
PROPERTIES OF MULTILAYERS OF  
POLY[2-(DIMETHYLAMINO)ETHYL METHACRYLATE-*b*-POLY(2-  
(DIETHYLAMINO)ETHYL METHACRYLATE)] MICELLES  
AND POLY(SODIUM 4-STYRENESULFONATE)

A THESIS SUBMITTED TO  
THE GRADUATE SCHOOL OF NATURAL AND APPLIED SCIENCES  
OF  
MIDDLE EAST TECHNICAL UNIVERSITY

BY

DİLARA GÜNDOĞDU

IN PARTIAL FULFILLMENT OF THE REQUIREMENTS  
FOR  
THE DEGREE OF MASTER OF SCIENCE  
IN  
CHEMISTRY

JANUARY 2017



Approval of the thesis:

**EFFECT OF FILM DEPOSITION CONDITIONS ON THE  
PROPERTIES OF MULTILAYERS OF  
POLY[2-(DIMETHYLAMINO)ETHYL METHACRYLATE-*b*-POLY(2-  
(DIETHYLAMINO)ETHYL METHACRYLATE)] MICELLES  
AND POLY(SODIUM 4-STYRENESULFONATE)**

submitted by **DİLARA GÜNDOĞDU** in partial fulfillment of the requirements for  
the degree of **Master of Science in Chemistry Department, Middle East  
Technical University** by,

Prof. Dr. Gülbin Dural Ünver  
Dean, Graduate School of **Natural and Applied Sciences**

\_\_\_\_\_

Prof. Dr. Cihangir Tanyeli  
Head of Department, **Chemistry**

\_\_\_\_\_

Assoc. Prof. Dr. İrem Erel Göktepe  
Supervisor, **Chemistry Dept., METU**

\_\_\_\_\_

**Examining Committee Members:**

Prof. Dr. Ali Gökmen  
Chemistry Dept., METU

\_\_\_\_\_

Assoc. Prof. Dr. İrem Erel Göktepe  
Chemistry Dept., METU

\_\_\_\_\_

Assoc. Prof. Dr. Ali Çırpan  
Chemistry Dept., METU

\_\_\_\_\_

Assoc. Prof. Dr. Eda Ayşe Aksoy  
Basic Pharmaceutical Sciences Dept., Hacettepe University

\_\_\_\_\_

Assist. Prof. Dr. Demet Asil Alptekin  
Chemistry Dept., METU

\_\_\_\_\_

**Date:** 26.01.2017

**I hereby declare that all information in this document has been obtained and presented in accordance with academic rules and ethical conduct. I also declare that, as required by these rules and conduct, I have fully cited and referenced all material and results that are not original to this work.**

Name, Last name: Dilara GÜNDOĞDU

Signature:

## ABSTRACT

### EFFECT OF FILM DEPOSITION CONDITIONS ON THE PROPERTIES OF MULTILAYERS OF POLY[2-(DIMETHYLAMINO)ETHYL METHACRYLATE-*b*-POLY(2- (DIETHYLAMINO)ETHYL METHACRYLATE)] MICELLES AND POLY(SODIUM 4-STYRENESULFONATE)

Gündoğdu, Dilara

M.Sc., Department of Chemistry

Supervisor: Assoc. Prof. Dr. İrem Erel Göktepe

January 2017, 67 pages

Block copolymer micelles (BCMs) are ideal drug carriers due to their hydrophobic core regions which can encapsulate water insoluble drug molecules. BCMs with stimuli-responsive cores are of specific interest due to release of the cargo by simply changing the environmental conditions, e.g. pH, temperature, ionic strength. Incorporation of BCMs into layer-by-layer (LbL) films is important to keep the BCMs stable in bloodstream and prevent the release of the cargo at an early stage. In addition, BCMs increase the loading capacity of the LbL films for functional hydrophobic molecules.

In this study poly[2-(dimethylamino)ethyl methacrylate-*b*-poly(2-(diethylamino)ethyl methacrylate)] (PDMA-*b*-PDEA) micelles with pH/temperature responsive PDMA-coronae and pH-responsive PDEA-core structure were used as building blocks to construct LbL films using poly(sodium 4-styrenesulfonate) (PSS) as the polymer counterpart. The effect of film deposition pH and temperature on the properties of the multilayers was investigated in detail. It was found that only 0.5-unit difference in the pH of polymer solutions resulted in a significant difference in the stability of the multilayers in the pH-scale. It was also demonstrated that the

effect of film deposition temperature on the properties of the resulting films were highly pH-dependent.

Results obtained in this thesis study contribute to the fundamental knowledge about the effect of film deposition conditions on the properties of multilayer films of a dually responsive BCM.

**Keywords:** Block copolymer micelles, Layer-by-layer films, Stimuli-responsive micelles

## ÖZ

### FİLM KAPLAMA KOŞULLARININ POLİ[2-(DİMETİLAMİNO)ETİL METAKRİLAT-*b*-POLİ(2- (DİETİLAMİNO)ETİL METAKRİLAT)] MİSELLER/POLİ(SODYUM 4- STİREN SÜLFONAT) ÇOK-KATMANLI FİMLERİNİN ÖZELLİKLERİNE ETKİSİ

Gündoğdu, Dilara

Yüksek Lisans, Kimya Bölümü

Tez Yöneticisi: Doç. Dr. İrem Erel Göktepe

Ocak 2017, 67 sayfa

Blok kopolimer miseller (BCM) hidrofobik çekirdek bölgelerinde suda çözünmeyen ilaçları barındırabildikleri için ideal ilaç taşıyıcılarıdır. BCM'lerin çekirdek bölgesini oluşturan bloğun ortam koşullarına duyarlı olması durumunda ise işlevsel moleküllerin salımı pH, sıcaklık, iyon şiddeti gibi çevre şartları değiştirilerek gerçekleştirilebileceğinden bu tip BCM'ler araştırmacıların özellikle ilgisini çekmektedir. BCM'lerin katman-katman (LbL) filmlerin içerisine yerleştirilmesi BCM'lerin kan dolaşımı içerisinde kararlılıklarının artması ve çekirdek bölgelerinde barındırdıkları kargonun erken salımını engellemek için önemlidir. Ayrıca, BCM'ler katman-katman filmlerin işlevsel hidrofobik molekülleri yükleme kapasitelerini de artırır.

Bu çalışmada, pH/sıcaklığa duyarlı PDMA-kabuk ve pH'a duyarlı PDEA-çekirdek yapısına sahip poli[2-(dimetilamino)etil metakrilat-*b*-poli(2-(dietilamino)etil metakrilat)] (PDMA-*b*-PDEA) miseller, PSS kullanarak LbL filmlerin hazırlanmasında yapıtaşı olarak kullanıldı. Film biriktirme pH'ı ve sıcaklığının çok-katmanlı filmlerin özelliklerine etkisi detaylı bir şekilde incelendi. Polimer çözeltilerinin pH'larındaki sadece 0.5 birimlik bir farkın çok-katmanlı filmlerin pH

kararlılıklarında belirgin bir farka yol açtığı anlaşıldı. Film kaplama sıcaklığının filmlerin özellikleri üzerindeki etkisinin de pH'a bağlı olduğu gösterildi.

Bu tez çalışmasında alınan sonuçlar, film kaplama koşullarının çifte duyarlı blok kopolimer misellerden hazırlanmış çok-katmanlı filmlerin özelliklerine etkisi üzerine temel bilgi birikimi oluşturulmasına katkıda bulunmuştur.

**Anahtar Kelimeler:** Blok kopolimer miseller, Katman-katman filmler, Uyarıcıya duyarlı miseller



*To My Beautiful Family...*

## ACKNOWLEDGEMENTS

First and foremost, I would like to thank my supervisor, Assoc. Prof. Dr. İrem Erel Göktepe for the valuable guidance and advice throughout the course of this work. Her kind but consistent attitude through the study thought me to research, to analyze, to interpret the results and solve the problems. I believe that knowledge and experience I gained through master prepared me for future academic steps thanks to her. Special thanks to Assoc. Prof. Dr. Ali Çırpan for allowing me to use their instrument and his research group for their kind support through measurements.

I would like to thank my lab members, for their unconditional friendship to Cansu Üstođlu and Meltem Haktanıyan, to Bora Onat for all valuable answers to my infinitely many questions without getting bored, to Eda Çađlı for her endless support and help, for the enjoyable times to Süleyman Atilla, finally to Majid Akbar for just being there through the long experiment hours.

My appreciation and gratitude go to the many friends, for their encouragement and support. Special thanks to lifelong friends, Gökçe Çalış who helped me through the hardest times and laughed with me after, to Dilan Aslan and Ceren Soysal who were always been there for me, to Belgin Şahin and Melike Belli who provided full support from overseas places, to Ayşenur Seyrekbasan who tried to enlighten me with her research experience, to Direniş Çaylı, Elif Saka and Bike Özdemir for reminding me that true friends never break the bond.

Last but not least, I would like to thank my family who have always been there for me; to my mother Nurhan, my father Ali Rıza and my sister Nergis for their unconditional love, warm affection, endless understanding, and support.

## TABLE OF CONTENTS

ABSTRACT .....	v
ÖZ .....	vii
ACKNOWLEDGEMENTS .....	x
LIST OF FIGURES .....	xiv
LIST OF TABLES .....	xvii
LIST OF SCHEMES .....	xviii
LIST OF ABBREVIATIONS .....	xix
CHAPTERS	
1. INTRODUCTION .....	1
1.1 Stimuli-Responsive Polymers .....	1
1.1.1 Temperature-Responsive Polymers .....	1
1.1.1.1 LCST-Type Behavior .....	2
1.1.2 pH-Responsive Polymers .....	3
1.2 Stimuli-Responsive Block Copolymer Micelles (BCMs).....	4
1.2.1 Micellization of Stimuli-Responsive Double-Hydrophilic Block Copolymers .....	5
1.2.1.1 pH-Induced Micellization .....	6
1.2.1.2 Temperature-Induced Micellization.....	8
1.3 Layer-by-Layer Self Assembly Technique .....	9
1.3.1 Stimuli-Responsive LbL Films .....	11

1.3.1.1	pH-Responsive LbL Films .....	11
1.3.1.2	Temperature-Responsive LbL Films.....	13
1.4	Aim of the Thesis .....	16
2.	EXPERIMENTAL .....	17
2.1	Materials.....	17
2.2	Instrumentation.....	19
2.3	Preparation of (PDMA- <i>b</i> -PDEA) Micelles .....	20
2.4	Loading Pyrene to (PDMA- <i>b</i> -PDEA) Micelles .....	20
2.5	Preparation of Multilayers of PSS / PDMA- <i>b</i> -PDEA Micelles .....	20
2.6	pH-stability of the Multilayers .....	21
2.7	Release of Pyrene from Multilayers.....	21
3.	RESULTS AND DISCUSSION .....	23
3.1	pH-Induced Micellization of PDMA- <i>b</i> -PDEA .....	23
3.2	pH-Dependent Thermo-Responsive Behavior of PDMA- <i>b</i> -PDEA Micelles... ..	26
3.3	Multilayers of PSS and PDMA- <i>b</i> -PDEA Micelles .....	29
3.3.1	Effect of Deposition pH on LbL Growth .....	30
3.3.2	Effect of Deposition Temperature on LbL Growth.....	34
3.4	pH-Stability of Multilayers of PDMA- <i>b</i> -PDEA Micelles and PSS .....	38
3.4.1	Effect of Film Deposition pH on the pH-Stability of Multilayers .....	38
3.4.2	Effect of Post-assembly Temperature on the pH-stability of Multilayers... ..	42
3.4.3	Effect of Film Deposition Temperature on the pH-Stability of Multilayers .....	44
3.5	Long-Term pH-Stability of the Multilayers .....	46

3.6	pH-Induced Release of Pyrene from the Multilayers.....	47
3.6.1	Pyrene Loading into (PDMA- <i>b</i> -PDEA) Micelles.....	47
3.6.2	Pyrene Release from the Surface .....	49
4.	CONCLUSION .....	53
	REFERENCES.....	55

## LIST OF FIGURES

### FIGURES

- Figure 1.** Phase diagrams of the polymers having LCST (left) and UCST (right). Green line shows boundary of phase separation. Modified from Gibson and O'Reilly Chem. Soc. Rev. (2013) [13] .....2
- Figure 2.** Schematic representation of coil-to-globule transition of a polymer exhibiting LCST. Modified from Molinaro et al., Biomaterials (2002) [16]. .....3
- Figure 3.** Schematic representation of ionization of PAA with increasing pH. Modified from Chan et al., Adv. Drug Deliv. Rev. (2013) [18].....3
- Figure 4.** Schematic representation of deionization of PDEA with increasing pH. Modified from Chan et al., Adv. Drug Deliv. Rev. (2013) [18].....4
- Figure 5.** Reversible unimer-to-micelle transition of a double hydrophilic block copolymer under the effect of stimuli. Modified from Lazzari et al., Block copolymers in nanoscience, 2006 [40]. .....5
- Figure 6.** pH-induced Micellization of PSSNa-*b*-PSCOONa. Modified from Gabaston et al.; Polymer (1999) [45]. ..... 7
- Figure 7.** Schematic representation of swelling of (PAH/PSS) multilayers in basic conditions due to the unbalanced electric charges. Modified from Đjugnat and Sukhorukov, Langmuir (2004) [65]..... 11
- Figure 8.** Hydrodynamic size as a function of pH (Panel A); size distribution curves of PDMA-*b*-PDEA at 25°C, at pH 3 and pH 7.5 (Panel B).....24

<b>Figure 9.</b> Zeta potential of PDMA- <i>b</i> -PDEA as a function of pH.....	25
<b>Figure 10.</b> TEM image of 1mg/ml PDMA- <i>b</i> -PDEA micelle solution at pH 8, 25°C. .....	26
<b>Figure 11.</b> Hydrodynamic size of PDMA- <i>b</i> -PDEA micelles as a function of temperature and the size distributions of PDMA- <i>b</i> -PDEA micelles by number with increasing temperature at pH 7.5 (A), pH 8 (B), pH 8.5 (C). .....	29
<b>Figure 12.</b> Effect of deposition pH on the multilayer growth of PSS and PDMA- <i>b</i> - PDEA micelles at 25°C. ....	32
<b>Figure 13.</b> Multilayer growth at 30°C at pH 8 (Panel A) and pH 8.5 (Panel B). The data obtained at 25°C is plotted for comparison.....	35
<b>Figure 14.</b> Comparison of the thickness of a 12-layer PDMA- <i>b</i> -PDEA micelles/PSS deposited under different pH and temperature conditions.....	37
<b>Figure 15.</b> Fraction retained at the surface after exposure to PBS solutions of decreasing pH at 25°C for multilayers constructed at pH 8 or pH 8.5, at 25°C. ....	39
<b>Figure 16.</b> AFM, topography images (10 μm x 10 μm) of 20 bilayer PSS/ PDMA- <i>b</i> - PDEA film deposited at pH 8, 25°C (Panel A) and film immersed into PBS solution at pH 6, 25°C for 6 hours (Panel B).....	41
<b>Figure 17.</b> Fraction retained at the surface after exposure to PBS solutions of decreasing pH at 37.5°C for multilayers constructed at pH 8 or pH 8.5, at 25°C. ....	42

<b>Figure 18.</b> Fraction retained at surface after exposure to PBS solutions of decreasing pH at 25°C and 37.5 °C for multilayers constructed at pH 8 (Panel A) and pH 8.5 (Panel B) at 25 °C.....	43
<b>Figure 19.</b> Fraction retained at the surface when the multilayers constructed at pH 8, 25°C or pH 8, 30°C were exposed to PBS solutions of decreasing pH at 25°C. ....	44
<b>Figure 20.</b> Fraction retained at the surface when the multilayers constructed at pH 8, 25°C or pH 8, 30°C were exposed to PBS solutions of decreasing pH at 37.5°C (Panel A). pH-stability profiles of the films constructed at 30 °C and exposed to PBS solutions with decreasing pH at 25 °C and 37.5 °C (Panel B). ....	46
<b>Figure 21.</b> Fraction retained at the surface at pH 6 at 25°C and 37.5 °C after 8.5 hours. Grey columns represent the multilayers before immersion into PBS solution. Red and blue column represent the multilayers after immersion into PBS solution for 8.5 hours at pH 6, 25°C and pH6, 37.5°C respectively. ....	47
<b>Figure 22</b> Fluorescence spectra of pyrene solution in the presence of PDMA- <i>b</i> -PDEA at pH 3 and pH 8. ....	49
<b>Figure 23.</b> Release of pyrene from the multilayers at pH 6 at either 25°C and 37.5°C. Release at pH 8 is plotted for comparison. ....	51



## LIST OF TABLES

### TABLES

<b>Table 1.</b> Chemical Structures of Polymers and Pyrene .....	18
--	----

## LIST OF SCHEMES

### SCHEMES

- Scheme 1.** Schematic representation of pH-induced micellization of PDMA-*b*-PDEA.....8
- Scheme 2.** LbL film preparation process by electrostatic attraction..... 10
- Scheme 3.** LbL film preparation process of PSS and PDMA-*b*-PDEA micelles .....30
- Scheme 4.** Schematic representation of multilayers deposited at pH 8 and pH 8.5 ..33
- Scheme 5.** Schematic representation of multilayers deposited at 25°C and 30°C. ....36
- Scheme 6.** Schematic representation of micelle disintegration and film disintegration for multilayers constructed at pH 8 and pH 8.5..... 40
- Scheme 7.** Schematic representation of loading of Pyrene molecules into the micelle core. ....48
- Scheme 8.** Schematic representation of disintegration of the micelles and pyrene release from the multilayers which immersed into PBS solution at pH 6... ..50

## LIST OF ABBREVIATIONS

<b>AFM</b>	Atomic Force Microscopy
<b>BCMs</b>	Block Copolymer Micelles
<b>BPEI</b>	Branched poly(ethyleneimine)
<b>DI</b>	Deionized
<b>DLS</b>	Dynamic Light Scattering
<b>DS</b>	Dextran sulfate
<b>IPEC</b>	Interpolyelectrolyte complexes
<b>LbL</b>	Layer-by- Layer
<b>LCST</b>	Lower Critical Solution Temperature
<b>Nano-ZS</b>	Nano-Zeta Sizer
<b>P2VP-<i>b</i>-PEO</b>	Poly(2-vinylpyridine)- <i>b</i> -poly(ethylene oxide)
<b>PAA</b>	Poly(acrylic acid)
<b>PAA-<i>b</i>-PDEAAm</b>	Poly(acrylic acid)- <i>b</i> - poly (N,N diethylacrylamide)
<b>PAH</b>	Poly(allylamine hydrochloride)
<b>PBS</b>	Phosphate Buffer Saline
<b>PDADMAC</b>	Poly(diallyldimethylammonium chloride)

<b>PDEA</b>	Poly(2-(diethylamino)ethyl methacrylate)
<b>PDMA</b>	Poly(2-(dimethylamino)ethyl methacrylate)
<b>PDMA-<i>b</i>-PDEA</b>	Poly[2(dimethylamino)ethylmethacrylate- <i>b</i> -poly(2-(diethylamino)ethyl methacrylate)]
<b>PEI</b>	Poly(ethyleneimine)
<b>PEMs</b>	Polyelectrolyte Multilayers
<b>PEO</b>	Poly(ethylene oxide)
<b>PLH</b>	Poly-L-histidin
<b>PMAA</b>	Poly(methacrylicacid)
<b>PMEMA-<i>b</i>-PDPA</b>	Poly[2-(N-morpholino)ethyl methacrylate- <i>block</i> -2-(diisopropyl amino)ethyl methacrylate]
<b>PMMA-<i>b</i>-PEO</b>	Poly(methacrylic acid)- <i>b</i> -poly(ethylene oxide)
<b>PNIPAAm-<i>b</i>-PMMA</b>	Poly(N-isopropylacrylamide- <i>b</i> -methyl methacrylate)
<b>PNIPAM</b>	Poly(N-isopropylacrylamide)
<b>PSS</b>	Poly(sodium 4-styrenesulfonate)
<b>PSS-<i>b</i>-PNIPAM</b>	Poly(styrenesulfonate)- <i>b</i> -poly(N-isopropylacrylamide)
<b>PSSNa-<i>b</i>-PSCoONa</b>	Poly(sodium 4-styrene sulfonate)- <i>b</i> -poly(sodium styrene carboxylate)
<b>PVPON-<i>b</i>-PNIPAM</b>	Poly(N-vinyl pyrrolidone)- <i>block</i> -poly(N-isopropyl acryl amide)

<b>PVS</b>	Poly(vinyl sulfate)
<b>TA</b>	Tannic acid
<b>TEM</b>	Transmission Electron Microscopy
<b>UCST</b>	Upper Critical Solution Temperature
<b><math>\beta</math>PDMA-<i>b</i>-PDPA</b>	Poly[3-dimethyl (methacryloyloxyethyl) ammonium propane sulfonate]- <i>block</i> -poly[2-(diisopropylamino)ethyl methacrylate]



## CHAPTER 1

### INTRODUCTION

#### 1.1 Stimuli-Responsive Polymers

Stimuli responsive polymers can change their properties such as solubility, volume, conformation, phase, shape etc. when exposed to different stimuli, e.g. light, temperature, pH, solvent composition, electric field, etc. [1,2]. Stimuli responsive polymers are used in a wide range of application areas such as controlled drug delivery, bio-separation, protein purification, personal care, industrial coatings, oil exploration, biological and membrane science, viscosity modifiers, colloid stabilization, surface modification and water remediation [3]. pH and temperature are two of the most extensively studied stimuli in biomedical applications.

##### 1.1.1 Temperature-Responsive Polymers

Thermo-responsive polymers are widely used in biomedical applications, e.g. tissue engineering, drug and gene delivery [4–7]. Change in temperature causes a rapid change in the solubility of thermo-responsive polymers [2]. They show temperature dependent, reversible sol-gel transitions. [8]. The temperature at which the phase transition is observed is related to the ratio of the hydrophilic and hydrophobic parts on the polymer chain [2]. Thermo-responsive polymers can be grouped into two: i) polymers exhibiting lower critical solution temperature (LCST) and ii) polymers exhibiting upper critical solution temperature (UCST) [9–11]. Polymers exhibiting LCST show phase separation upon heating while polymers with UCST show phase separation upon cooling (Fig. 1) [12].

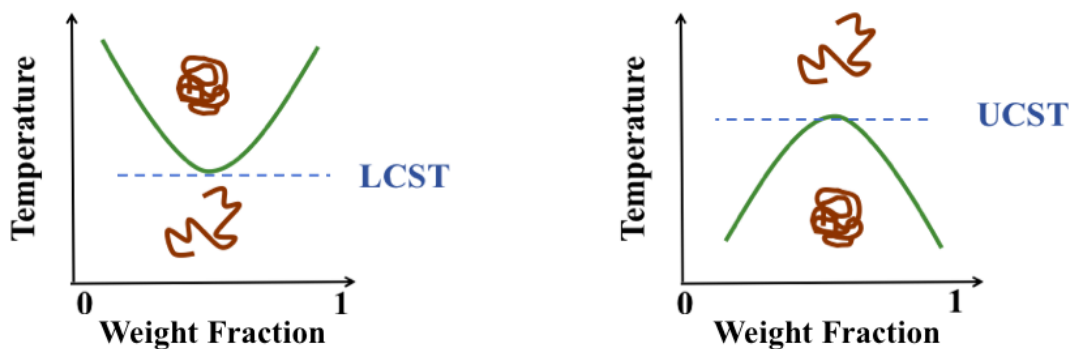


**Figure 1.** Phase diagrams of the polymers having LCST (left) and UCST (right). Green line shows boundary of phase separation. Modified from Gibson and O'Reilly Chem. Soc. Rev. (2013) [13]

#### 1.1.1.1 LCST-Type Behavior

Polymers exhibiting LCST-type phase behavior in aqueous environment is soluble in water below LCST but undergo a phase separation above this temperature. Below LCST, polymers generally form hydrogen bonds with water molecules surrounding them. As the temperature approaches LCST, hydrogen bonding interactions among the polymer chains and water molecules are partially disrupted and the polymer goes into a conformational transition from extended to globular coil (Fig. 2). At a certain temperature, so called LCST, the polymer-polymer interactions overcome the polymer-solvent interactions and subsequent aggregation of polymer is observed [14,15]. The most commonly studied thermo-responsive polymers showing LCST-type phase behavior are poly(N-isopropylacrylamide) (PNIPAM), poly(N,N-diethylacrylamide), poly(N-vinylalkylamide), poly(N-vinylcaprolactam) etc. [9].



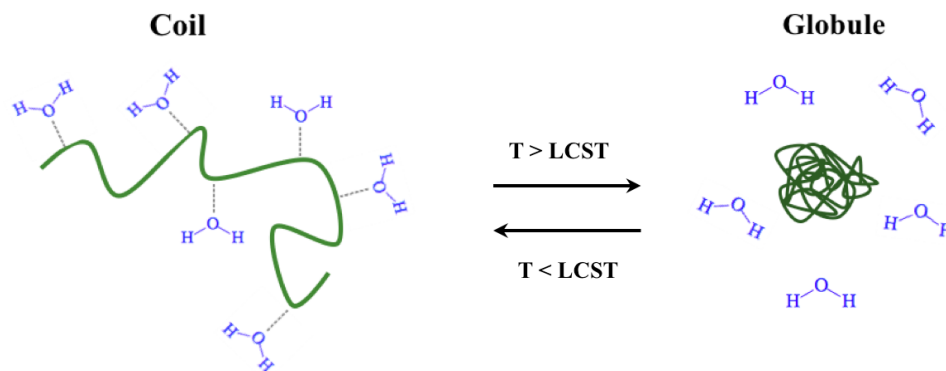


**Figure 2.** Schematic representation of coil-to-globule transition of a polymer exhibiting LCST. Modified from Molinaro et al., *Biomaterials* (2002) [16].

### 1.1.2 pH-Responsive Polymers

pH-responsive polymers give response to pH changes by changing its solubility and conformation [17]. pH-responsive polymers have acidic or basic functional groups that ionize (protonate or deprotonate) depending on the solution pH [18]. Polymers possessing pH-dependent ionizable groups are also known as weak polyacids and weak polybases [2]. Poly(acrylic acid) (PAA) and poly(methacrylic acid) (PMAA) are commonly used weak polyacids [19,20]. For example, carboxylic acid groups of PAA deprotonates at pH values above its  $pK_a$  of 4.25 (Fig 3.) [18] and the electrostatic repulsion among the ionizable groups causes swelling of PAA in water [21,22].

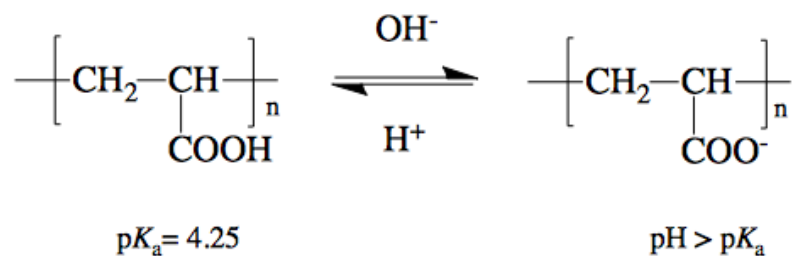


**Figure 3.** Schematic representation of ionization of PAA with increasing pH. Modified from Chan et al., *Adv. Drug Deliv. Rev.* (2013) [18].

Poly(2-diethylaminoethyl methacrylate) (PDEA) is an example of a commonly used weak polybase. Tertiary amine groups of PDEA are protonated at pH values below its  $pK_a$  of 7.3 [23]. PDEA deprotonates above its  $pK_a$  and becomes water-insoluble (Fig. 4).

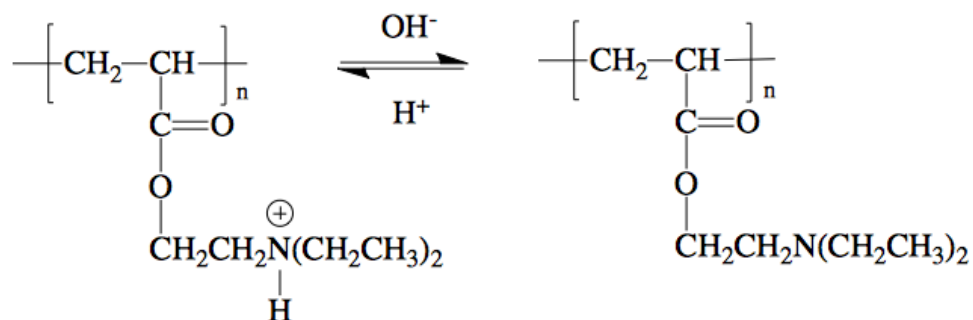


**Figure 4.** Schematic representation of deionization of PDEA with increasing pH.

Modified from Chan et al., *Adv. Drug Deliv. Rev.* (2013) [18].

## 1.2 Stimuli-Responsive Block Copolymer Micelles (BCMs)

BCMs are good candidates for cancer treatment due to encapsulation of drug molecules into the stimuli-responsive micellar cores. Chemotherapy is one of the treatment types to treat cancer. However, common chemotherapy treatments depend on anticancer drug molecules that damage both tumors and healthy tissues on human body [24,25]. Additionally, anticancer drug molecules cannot work effectively due to distribution of the drugs to the undesired organs, poor cellular uptake, and incapability of targeting required locations [26,27]. Multifunctional polymer systems that are capable of targeting tumor sites and releasing drug molecules in a controlled manner have attracted great attention to overcome these obstacles [28–32]. Amphiphilic block copolymers with both hydrophilic and hydrophobic blocks are capable of producing self-assembled nanoaggregates under proper conditions. Such block copolymer micelles (BCMs) can encapsulate and release drug molecules in their hydrophobic cores. Using BCMs, it is possible to increase the solubility of the drug, enhance drug efficacy and decrease the drug toxicity [33]. BCMs have been widely used in nanomedicine since they provide targeted and controlled drug release.

Besides, they have higher blood circulation time for drugs [34,35]. Among many different types of micellar aggregates, BCMs with pH- and/or temperature-responsive cores are of specific interest due to difference in acidity and temperature between the tumor tissues and normal healthy ones [36,37]. Stimuli-responsive BCMs exhibit structural changes or disassemble under proper stimuli (pH, temperature etc.) by releasing the drug at specific locations and providing a local treatment [33].

### 1.2.1 Micellization of Stimuli-Responsive Double-Hydrophilic Block Copolymers

BCMs can be obtained from double hydrophilic block copolymers when either of the blocks is made water-insoluble by changing environmental conditions, e.g. temperature, pH, ionic strength etc. [38,39]. The hydrophobic-hydrophobic interactions among the water-insoluble blocks induces the self-assembly in solution and formation of BCMs. In general, unimer-to-micelle formation is reversible for BCMs of double hydrophilic block copolymers. BCMs turn into unimer form when the stimuli is removed [40]. Figure 5 demonstrates the unimer-to-micelle transition.

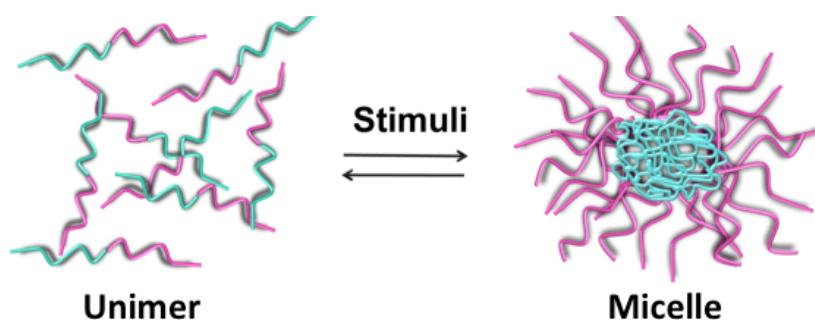


**Figure 5.** Reversible unimer-to-micelle transition of a double hydrophilic block copolymer under the effect of stimuli. Modified from Lazzari et al., Block copolymers in nanoscience, 2006 [40].

### 1.2.1.1 pH-Induced Micellization

Double hydrophilic block copolymers composed of at least one polyacid or polybase block can form BCMS when the pH-sensitive block is made water-insoluble above/below the  $pK_a$  of the polybase/polyacid. The hydrophobic-hydrophobic interactions among the pH-sensitive blocks induces the formation of the micellar cores, while the other hydrophilic block constitutes the micellar coronae and assures the solubility of the micellar aggregates in aqueous environment. The resulting nanostructures have core-shell structures.

For example, poly(2-vinylpyridine-*b*-ethylene oxide) (P2VP-*b*-PEO) dissolve at acidic pH. P2VP-*b*-PEO unimers transform into P2VP-*b*-PEO micelles with P2VP-core and PEO-corona at pH values above the  $pK_a$  of P2VP ( $pK_a$ ; 3.5-4.5 [41]). The driving force for micellization is the deprotonation of P2VP block and the aggregation of P2VP units, forming the micellar cores [42]. Formation of P2VP-*b*-PEO micelles is reversible. P2VP-*b*-PEO micelles dissolve below pH 5 upon protonation of the P2VP units.

In another study Gohy et al. formed micelles of interpolyelectrolyte complexes (IPEC) by mixing poly(methacrylic acid)-*b*-poly-(ethylene oxide) PMAA-*b*-PEO and P2VP-*b*-PEO diblock copolymers, in a restricted range of pH ( $2 < \text{pH} < 6$ ) [43]. Micelles contains IPEC core made by association of PMAA ( $pK_a$ ; 5.6 [44]) and P2VP ( $pK_a$ ; 3.5-4.5) blocks and a corona of PEO blocks. In this pH range, PMAA groups are negatively charged due to deprotonation in contrast P2VP is positively charged due to protonation. Negatively charged PMAA and positively charged P2VP forms interpolyelectrolyte core in this pH range. They produced spherical shaped large micelles by mixing ionized oppositely charged blocks.

Both of the examples mentioned above had hydrophilic and neutral coronae. BCMS can also be obtained from block copolymers composed of two ionizable blocks.

For example, poly(sodium-4-styrene sulfonate)-*b*-poly(sodium styrene carboxylate) (PSSNa-*b*-PSCoONa) forms micelles at pH lower than the  $pK_a$  of PSCoOH ( $pK_a$  ~4.4). The resulting nanoaggregates had PSCoOH-core and PSSNa-corona. Note that,  $pK_a$  of PSSNa is smaller than 1, therefore PSSNa is in the ionized form in a

wide pH range and assure the solubility of PSSNa-*b*-PSCoONa micelles in aqueous environment [45]. Figure 6 demonstrates the formation of PSSNa-*b*-PSCoONa micelles.

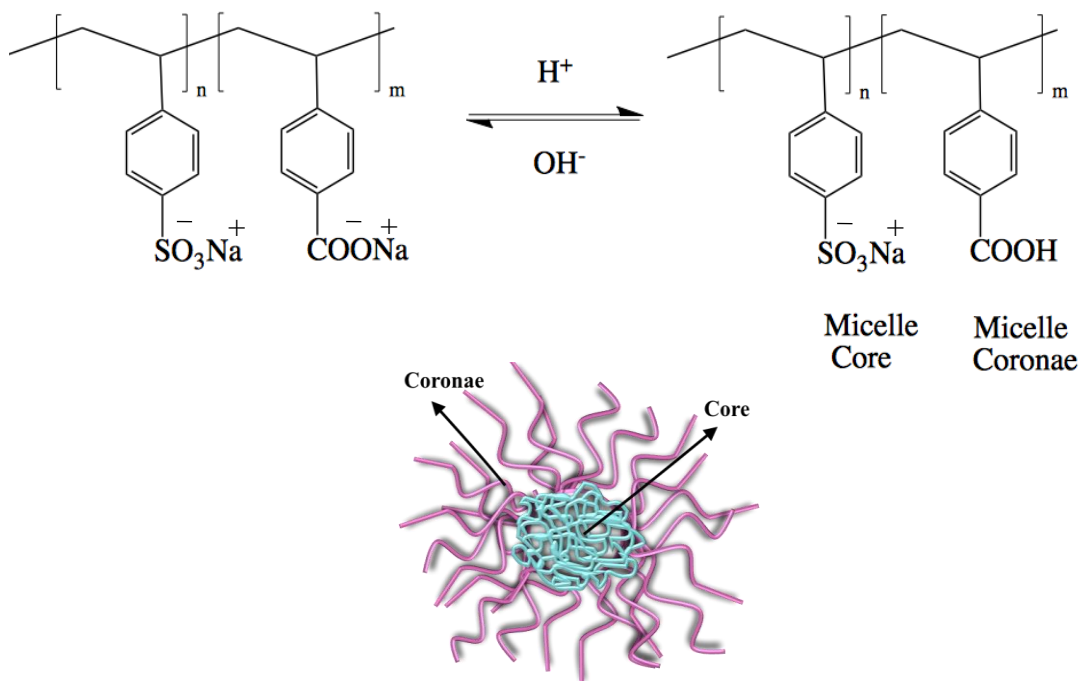
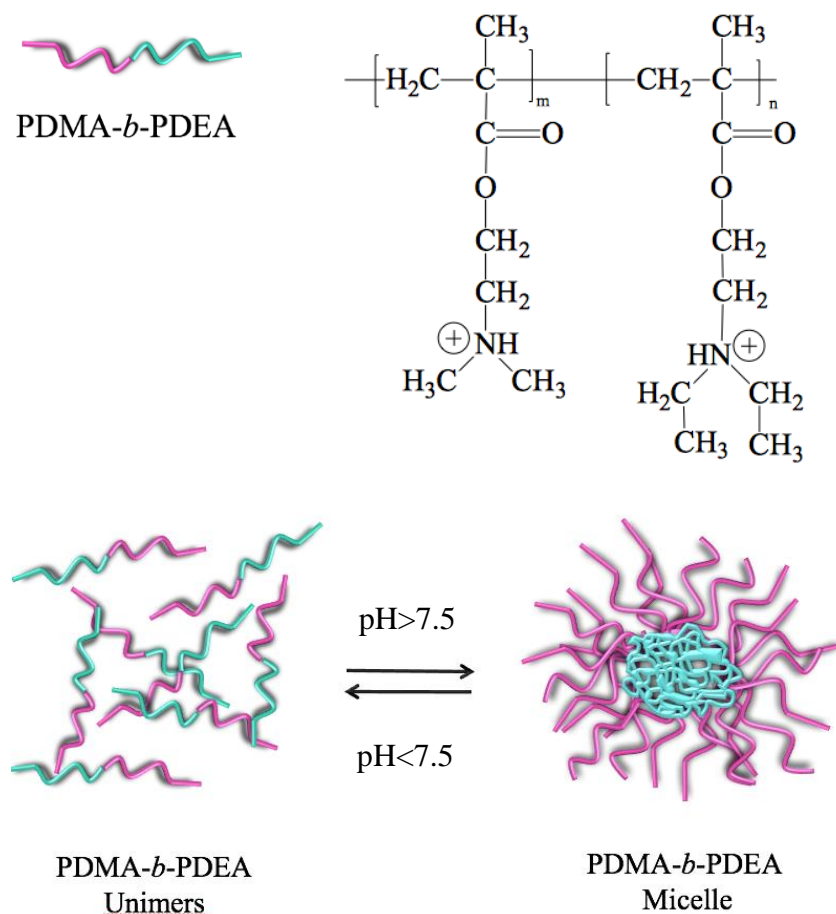


**Figure 6.** pH-induced Micellization of PSSNa-*b*-PSCoONa. Modified from Gabaston et al.; Polymer (1999) [45].

Another example of a double hydrophilic block copolymer with two ionizable blocks is poly[2-(dimethylamino)ethyl methacrylate-*b*-poly(2-diethylamino)ethyl methacrylate] (PDMA-*b*-PDEA). PDMA-*b*-PDEA has two polybasic blocks. PDMA has a  $pK_a$  of 7.0 and PDEA has a  $pK_a$  of 7.3 [23]. At  $\text{pH} < 7.5$ , PDMA-*b*-PDEA dissolved molecularly in aqueous solution. Above  $\text{pH} 7.5$ , PDMA-*b*-PDEA self-assembles into PDMA-*b*-PDEA micelles with PDEA-core and PDMA-coronae. Interestingly, the amino groups on both PDEA and PDMA unprotonate as the pH is increased. However, PDMA which is more hydrophilic than PDEA remains its solubility in water at pH values even above its  $pK_a$ . Therefore, the more hydrophobic PDEA forms the micellar cores, while the hydrophilic PDMA forms the coronae and

assures the stability in water [46]. Scheme 1 demonstrates the unimer-to-micelle transition of PDMA-*b*-PDEA.



**Scheme 1.** Schematic representation of pH-induced micellization of PDMA-*b*-PDEA.

### 1.2.1.2 Temperature-Induced Micellization

Micellization of double-hydrophilic block copolymers in aqueous media can be triggered by temperature when one of the blocks exhibits LCST property. At temperatures lower than LCST, thermosensitive block copolymers dissolve completely in water, while formation of micelle is observed at temperatures higher than LCST. [39]

For instance, Müller and co-workers displayed that above the LCST of PDEAAm

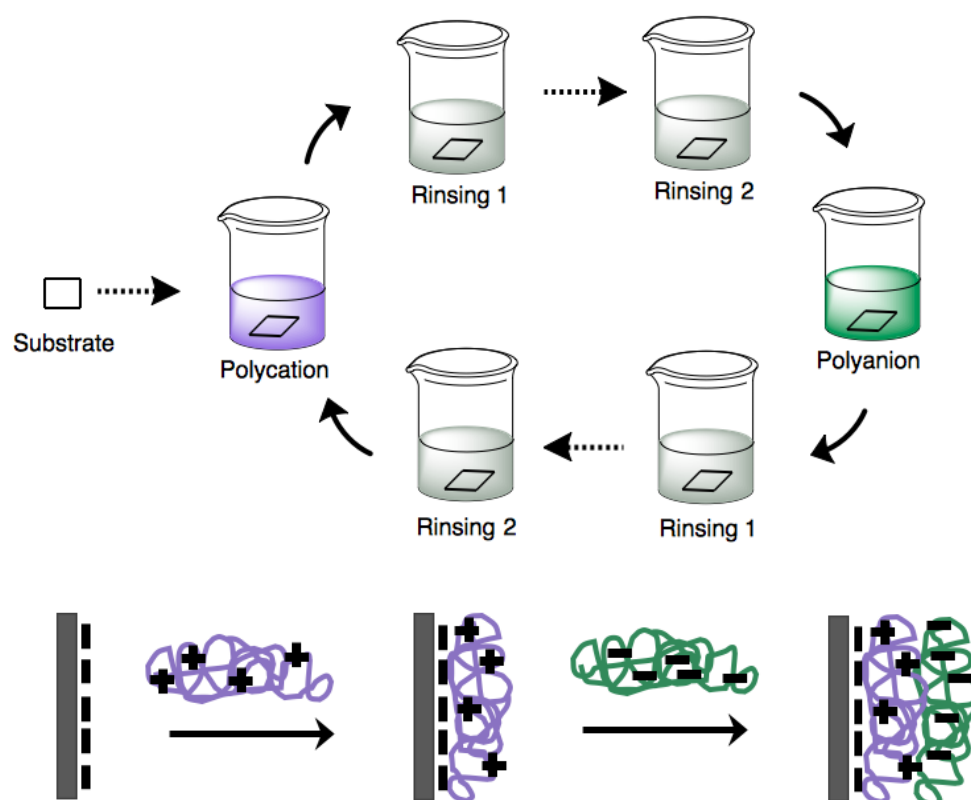
which is 35 °C at basic conditions, micelles of poly(acrylic acid)-*block*-poly(N,N diethylacrylamide) (PAA-*b*-PDEAAm) with PAA-corona and PDEAAm-cores were prepared. However, below 35 °C, disintegration of PAA-*b*-PDEAAm micelles were observed at basic conditions. This block copolymer gives response to both pH and temperature in aqueous solution due to pH-responsive PAA block ( $pK_a$ ; 4.25) and temperature-responsive PDEAAm block. At basic conditions, above LCST of PDEAAm block, micelles are formed with PDEAAm-core and PAA-coronae. In contrast, at acidic conditions, below LCST micelles are formed with an expanded PAA-core due to protonation of PAA block at  $pH < pK_a$  [47].

In another study related to temperature-triggered block copolymer micellization, Wei et al. formed poly(N-isopropylacrylamide-*b*-methyl methacrylate) (PNIPAAm-*b*-PMMA) micelles below LCST of PNIPAAm (26 °C), with hydrophobic core PMMA and hydrophilic corona PNIPAAm and they loaded drug (prednisone acetate) into the micellar cores. It was observed that the drug loaded nanoparticles were well dispersed in the distilled water at 26 °C but aggregated at 40 °C. Nanoparticles deformed and precipitated with the increase in temperature and release the enclosed drug [48].

### 1.3 Layer-by-Layer Self Assembly Technique

Layer-by-layer (LbL) self-assembly is an economic and easy way of producing ultra-thin polymer films. Scheme 2 shows LbL film assembly process. As seen in the scheme, the substrate is first immersed into positively charged polyelectrolyte solution for a given period of time. The polycation coated substrate is then rinsed using a buffer solution at the same pH with the polycation solution to remove the loosely bound polymers from the surface. The polycation coated and rinsed substrate is immersed into the polyanion solution and similarly, this step is also followed by a rinsing step using a buffer solution at the same pH with the polyanion solution. This cycle continues until one reaches the desired number of layers at the surface. LbL films can be constructed onto not only two- dimensional (2D) but also three-dimensional (3D) substrates [49–51].

The properties of multilayer films constructed via LbL technique can be simply controlled by adjusting the assembly and post-assembly conditions such as pH, temperature, ionic strength etc. [52–54]. The majority of the studies concerning LbL films are based on electrostatic multilayers in which the driving force for multilayer assembly is the electrostatic interactions among the layers. However, LbL films can also be constructed via hydrogen bonding [55,56], coordination bonding [57], charge-transfer [58], metal-ligand [59] and bio-specific [60] interactions among the layers.



**Scheme 2.** LbL film preparation process by electrostatic attraction.

LbL self-assembly technique which is a facile, robust, effective method to modify surfaces and gives nanoscale control in film properties finds applications in many different areas, e.g. preparation of biomaterials, biosensing, drug/gene delivery, tissue engineering, diagnostics, detection, electronics, energy, and optics [61–64].



### 1.3.1 Stimuli-Responsive LbL Films

#### 1.3.1.1 pH-Responsive LbL Films

LbL films of weak polyelectrolytes show response to pH variations. For example, Djugnat and Sukhorukov produced hollow micro capsules by depositing PSS/PAH multilayers onto  $\text{CaCO}_3$  and  $\text{MnCO}_3$  and then dissolving the  $\text{CaCO}_3$  and  $\text{MnCO}_3$  template using ethylenediaminetetraacetic acid (EDTA) and citric acid solutions respectively [65]. PSS is a strong polyanion and its charge density is not affected by the pH of the environment. In contrast, PAH is a weak polycation with a  $\text{p}K_a$  of 10.8. They demonstrated that PAH/PSS capsules swelled at basic conditions due to unprotonation of the primary amino groups on PAH and partial loss of electrostatic interaction among PAH and PSS. The free negatively charged units on PSS cause repulsion among the layers, resulting in an increase in osmotic pressure and swelling of the multilayer. Figure 7 shows the structural change within the PAH/PSS multilayers with increasing pH.

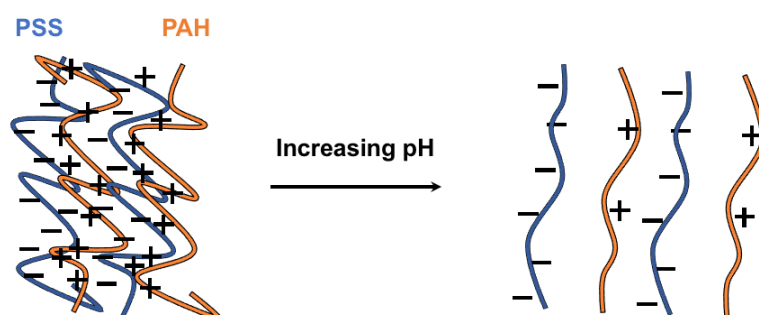


**Figure 7.** Schematic representation of swelling of (PAH/PSS) multilayers in basic conditions due to the unbalanced electric charges. Modified from Djugnat and Sukhorukov, Langmuir (2004) [65].

By taking advantage of pH-induced structural changes within the multilayers, it is possible to encapsulate and release functional molecules from the multilayers. For example, Chung and Rubner constructed multilayers of poly(allyl amine

hydrochloride) (PAH) and poly(acrylic acid) (PAA) at pH 2.5. At pH 2.5, PAH acts like a strong polyelectrolyte and it is fully charged. Unlike PAH, PAA with a  $pK_a$  of 5.5 is partially ionized at pH 2.5. Upon construction of the films, multilayers were exposed to methylene blue solution at pH 7. Note that, PAA further ionizes with increasing pH. Positively charged methylene blue was loaded into the multilayers via electrostatic interactions among methylene blue and negatively charged PAA. Methylene blue was released from the surface with decreasing pH due to protonation of carboxylic acid groups of PAA and loss of electrostatic interactions among PAA and methylene blue [66].

In another study, Anzai and co-workers prepared LbL films of insulin at acidic pH using a polyanion e.g. PAA, dextran sulfate (DS) and poly(vinyl sulfate) (PVS) through electrostatic interactions among the positively charged insulin and negatively charged polyanion. Insulin was released from the surface as the pH approached moderately acidic and neutral conditions due to decrease in the amount of positive charges on Insulin and loss of electrostatic interactions among Insulin and the polyanion within the multilayers [67].

Hydrogen-bonded multilayers have also been examined for controlled release of functional molecules from the surface due to pH-response of hydrogen-bonded multilayers at mild pH conditions. For example, Sukhishvili and co-workers demonstrated release of Rhodamine 6G from the multilayers. Multilayers of PEO and PMAA was constructed at strongly acidic conditions via hydrogen bonding interactions among PEO and PMAA. Rhodamine 6G was loaded into the multilayers at pH 4.2 when excess negative charge was created within the multilayers by increasing ionization of PMAA as the pH was increased. Rhodamine 6G was released from the surface by either decreasing or increasing pH. When the pH is decreased, PMMA protonates, thus the electrostatic interaction between PMAA and Rhodamine 6G is lost, resulting in release of Rhodamine 6G from the surface. When the pH is increased, Rhodamine 6G is released from the surface due to ionization of PMAA and loss of hydrogen bonding interactions among PEO and PMAA, resulting in disintegration of the multilayers [68].

As discussed earlier in Section 1.2, BCMs are ideal carriers for hydrophobic drug molecules. Incorporating BCMs into multilayer films are advantageous to increase the loading capacity of the multilayers for hydrophobic molecules as well as to increase the stability of BCMs in the blood stream. Erel et al. demonstrated pH-induced release of pyrene from multilayers of poly[2-(N-morpholino)ethyl methacrylate-*block*-2-(diisopropyl amino)ethyl methacrylate] (PMEMA-*b*-PDPA) micelles. Multilayers were constructed using pyrene loaded PMEMA-*b*-PDPA micelles at neutral conditions. It was shown that when the multilayers were exposed to moderately acidic conditions, pyrene could be released from the surface due to protonation of the amino groups on PDPA and dissolution of the micellar cores [69].

### 1.3.1.2 Temperature-Responsive LbL Films

The majority of the studies concerning temperature-responsive LbL films is based on multilayers containing PNIPAM due to LCST of PNIPAM which is very close to body temperature, making PNIPAM a promising material for biomedical applications. PNIPAM is a hydrogen accepting neutral polymer, therefore it can be incorporated into the multilayers via hydrogen bonding interactions using a hydrogen donating polymer. Alternatively, copolymers of PNIPAM can be prepared using a monomer with ionizable groups, so that charged units on the PNIPAM copolymer can form electrostatic interactions with a polymer counterpolymer and drive the LbL assembly.

Quinn and Caruso demonstrated the effect of temperature on the loading and release properties of PNIPAM containing multilayers. Multilayers of PNIPAM/PAA constructed at 30°C resulted in thicker and smoother films when compared to multilayers coated at 10°C or 21 °C. Lower roughness was obtained for films deposited at 30°C because PNIPAM conformation changes to tighter coil at temperatures close to its LCST, leading smoother films. They also found that loading and release of Rhodamine B from the films were reversible but showed differences when exposed to solutions at different temperatures. They followed the loading and release profiles of the dye from UV-visible spectrophotometry of a thin film on a

quartz slide. As temperature was increased higher amount of dye loaded and also higher amount of dye were released [70]

In another study, Klitzing and co-workers LbL deposited block copolymer of PNIPAM and PSS (PSS-*b*-PNIPAM) using positively charged poly(diallyldimethylammonium chloride) (PDADMAC) via electrostatic interactions among PSS and PDADMAC. Multilayers were exposed to a heating/cooling cycle. The thickness of the multilayers decreased upon heating due to the collapse of PNIPAM chains. They recorded a hysteresis on the thermal response during the cooling cycle which was correlated with the electrostatic association among the layers [71].

Sukhishvili and co-workers took advantage of LCST-type phase behavior of PNIPAM to produce BCMs with temperature-responsive cores. They demonstrated temperature-induced self-assembly of poly(N-vinyl pyrrolidone)-*block*-poly(N-isopropyl acryl amide) (PVPON-*b*-PNIPAM) and construction of multilayers above the LCST of PNIPAM. Multilayers of PVPON-*b*-PNIPAM micelles were capable of releasing Doxorubixin (DOX) from the surface when the temperature was below the LCST of PNIPAM due to dissolution of the PNIPAM micellar cores [72]

Sukhishvili and co-workers also demonstrated the temperature-induced micellization of poly(2-(dimethylamino)ethyl methacrylate)-*b*-poly-(N-isopropylacrylamide) (PDMA-*b*-PNIPAM) above the LCST of PNIPAM. PDMA-*b*-PNIPAM micelles with PNIPAM-core and PDMA-coronae were LbL deposited at the surface via electrostatic interactions among positively charged PDMA-coronae and negatively charged PSS. The temperature response of PDMA-*b*-PNIPAM micelles within the multilayers were examined in detail. They found that although dissolution of PNIPAM-micellar cores was prevented when PDMA-*b*-PNIPAM micelles were incorporated into the multilayers, pyrene release from the micellar cores could be tuned by temperature. They found that the rate of pyrene release was higher at temperatures below the LCST of PNIPAM than the rate of release at temperatures above the LCST of PNIPAM. This was correlated with the loss of hydrophobic-hydrophobic interactions among the PNIPAM and pyrene below the LCST of PNIPAM [73].

Recently, poly(2-alkyl-2-oxazoline)s have attracted attention of the researchers due to its LCST-type phase behavior and important biological properties such as biocompatibility, nontoxicity, anti-fouling [12,74]. The first study on LbL films of poly(2-alkyl-oxazoline)s was reported by Erel et al in which hydrogen accepting poly(2-isopropyl 2-oxazoline) was LbL deposited at the surface using hydrogen donating Tannic Acid (TA) [75] Later, De Geest and Hoogenboom and their co-workers have investigated the effect of assembly temperature on the mechanism of LbL growth of poly(n-propyl oxazoline) and TA [76]. In addition, in another study, they reported on the thermodynamics of the multilayer assembly of several different poly(2-alkyl-2-oxazoline)s and TA [77]

There are also studies concerning dual responsive multilayers. For example, Osypova et al. constructed multilayers of PAA-*b*-PNIPAM and PAH via electrostatic interactions among PAA and PAH. PNIPAM block of PAA-*b*-PNIPAM introduced temperature-response, whereas PAA block of PAA-*b*-PNIPAM and PAH introduced pH-response to the multilayers. They found that protein adsorption onto multilayers of PAA-*b*-PNIPAM and PAH was highly affected by the temperature and pH of the medium. They correlated this feature of the multilayers with the temperature-induced conformational changes in PNIPAM above its LCST and structural changes within the multilayers due to changes in the ionization of weak polyelectrolytes with changing pH. Structural changes on the film caused by protonation of PAA. When deprotonated, PAA interacts with PAH more strongly adapting flat configuration but protonated PAA results in lower ‘points’ of interaction with PAH and so-called loops and tails formation because of that multilayers show higher roughness. As a result, adsorption of protein onto multilayers affected by pH and temperature [78].

Erel et al. also reported on dual responsive LbL films. In one of the studies, with pH-responsive PDPA cores and temperature-responsive PMEMA corona was examined. It was found that as the temperature of the medium approached LCST of PMEMA, release of pyrene facilitated due to conformational changes within the multilayers arising from LCST-type phase behavior of PMEMA and formation of void-like structures within the multilayers [69].

In another study, Erel and co-workers examined LbL films of PSS and micellar complexes of poly[3-dimethyl (methacryloyloxyethyl) ammonium propane sulfonate]-*block*-poly[2-(diisopropylamino)ethyl methacrylate] ( $\beta$ PDMA-*b*-PDPA) micelles with pH-responsive PDPA-core and zwitterionic, temperature responsive  $\beta$ PDMA-coronae. They recorded swelling of the multilayers below the upper critical solution temperature (UCST) of  $\beta$ PDMA block and correlated this phenomenon with the conformational changes within the multilayers arising from UCST-type phase behavior of  $\beta$ PDMA block [79].

#### 1.4 Aim of the Thesis

In this thesis, the effect of film assembly pH and temperature on the pH stability of multilayers containing PDMA-*b*-PDEA micelles with dually responsive PDMA-coronae (pH- and temperature-responsive) and pH-responsive PDEA core structure were investigated.

There are studies concerning the aqueous solution properties of PDMA-*b*-PDEA micelles in the literature [46,80–83]. However, the number of studies concerning films of PDMA-*b*-PDEA micelles is limited. These studies reported on i) the effect of concentration and chain length on the pH-response of a monolayer of PDMA-*b*-PDEA micelles [84], ii) the adsorption kinetics of PDMA-*b*-PDEA micelles on silica/aqueous solution interface [85], iii) deposition of multilayers of nonquaternized or quaternized PDMA-*b*-PDEA micelles coated on polystyrene latex [86], silica nanoparticles [87,88] and iv) pH-induced reversible uptake and release of pyrene from a monolayer of PDMA-*b*-PDEA micelles adsorbed onto silica particles [89].

Different from above mentioned studies, this thesis aimed for the first time to investigate the effect of different multilayer assembly conditions on the pH-stability of multilayers of PDMA-*b*-PDEA micelles and PSS. Moreover, this thesis aimed to show the effect of pH on the temperature response properties of the multilayers. It was aimed to show the results within the context of pH-dependent LCST-type phase behavior of PDMA.

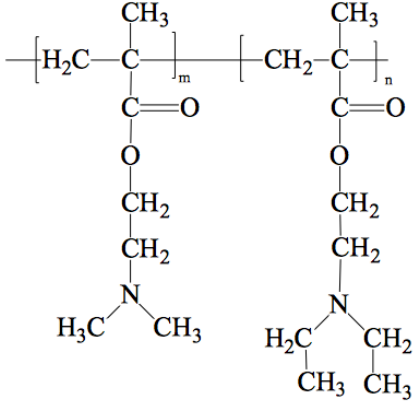
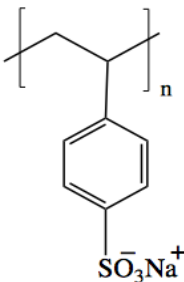
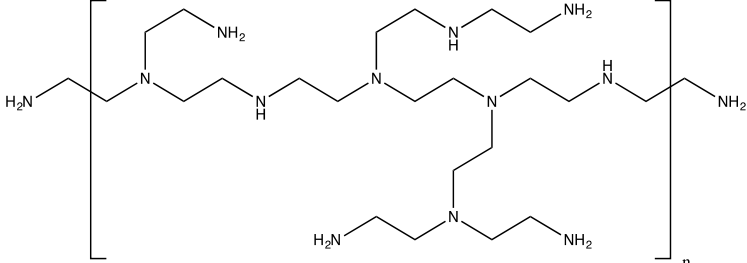
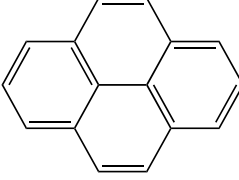
## CHAPTER 2

### EXPERIMENTAL

#### 2.1 Materials

Poly(sodium 4-styrenesulfonate) (PSS;  $M_w$ : 70,000), branched poly(ethyleneimine) (BPEI;  $M_w$ : 25,000), pyrene (98.0%), phosphate buffered saline (PBS); disodium hydrogen phosphate dehydrate ( $\text{Na}_2\text{HPO}_4 \cdot 2\text{H}_2\text{O}$ ), sodium hydroxide, hydrochloric acid and ethanol (99.8%) were purchased from Sigma-Aldrich Chemical Co. Sodium dihydrogen phosphate dihydrate ( $\text{NaH}_2\text{PO}_4 \cdot 2\text{H}_2\text{O}$ ), sulfuric acid (98%) were purchased from Merck Chemicals. The deionized (DI) water was purified by Milli-Q system (Millipore) at 18.2 M $\Omega$ . Poly[2-(dimethylamino)ethyl methacrylate-*block*-poly(2-diethylamino)ethyl methacrylate)] (PDMA<sub>72</sub>-*b*-PDEA<sub>60</sub> ;  $M_n$ : 23,700) was provided by Prof. Dr. Vural Bütün's Research Laboratory (Department of Chemistry, Eskişehir Osmangazi Üniversitesi). All materials and chemicals were used as received and DI water was used in all solutions.

**Table 1.** Chemical Structures of Polymers and Pyrene

Molecule	Chemical Structure
PDMA <sub>72</sub> - <i>b</i> -PDEA <sub>60</sub>	
PSS	
BPEI	
Pyrene	



## 2.2 Instrumentation

**Dynamic Light Scattering (DLS) and Zeta-potential Measurements:** Zetasizer Nano-ZS (Malvern Instruments Ltd., U.K.) was used to detect hydrodynamic size and zeta-potential of micelles. Hydrodynamic size of micelles were acquired by cumulants analysis of the autocorrelation data. Zeta-potential values were acquired via the Smoluchowski approximation from electrophoretic mobility data.

**Ellipsometry:** Ellipsometer of Optosense, USA (OPT-S6000) was used to detect film thickness.

**Fluorescence Spectroscopy:** Perkin Elmer LS55 Fluorescence Spectrometer was used in release studies of pyrene from the multilayers.

**Atomic Force Microscopy (AFM):** NT-MDT Solver P47 AFM was used to obtain information about the morphology of the multilayer films in tapping mode using Si cantilevers.

**Transmission Electron Microscopy (TEM):** TEM image was obtained using an FEI Tecnai G2 Spirit BioTwin CTEM operating at an acceleration voltage of 20–120 kV.

**pH Meter:** pH of solutions was adjusted by Starter 3000 bench pH meter throughout the study.

### **2.3 Preparation of (PDMA-*b*-PDEA) Micelles**

PDMA-*b*-PDEA was dissolved in 0.01 M NaH<sub>2</sub>PO<sub>4</sub> buffer at pH 2.5 with a final concentration of 1mg/mL. Solution pH was slowly increased above pH 7.5 on stirrer to induce micellization. 0.25 M NaOH solution was used between pH 2.5 –pH 7.5 and above pH 7.5 0.1 M NaOH solution was used to adjust pH of PDMA-*b*-PDEA solution.

### **2.4 Loading Pyrene to (PDMA-*b*-PDEA) Micelles**

Pyrene was dissolved in ethanol by 10 min sonication at a fixed concentration, after that 0.01 M NaH<sub>2</sub>PO<sub>4</sub> buffer at pH 2.5 was added to pyrene/ethanol solution to give a final concentration of  $7 \times 10^{-7}$  M. PDMA-*b*-PDEA was dissolved in this pyrene solution to give a final concentration 1 mg/mL and solution was left on stirrer overnight. Micelles are prepared adjusting the pH above 7.5 by adding NaOH solution as mentioned above and left on stirrer for overnight to load pyrene to the hydrophobic core of the PDMA-*b*-PDEA micelles.

### **2.5 Preparation of Multilayers of PSS / PDMA-*b*-PDEA Micelles**

Silicon wafers were treated with concentrated sulfuric acid by simply immersing into acid solution for 85 min and to get rid of the acid, they were rinsed with distilled and DI water for several minutes. Acid treated clean silicon wafers were then dried with compressed nitrogen gas flow. After acid treatment, silicon wafers were treated with 0.25 M NaOH solution for 10 minutes and rinsed and dried as described above. Before depositing the multilayers on the silicon wafers, precursor layers were prepared with 0.8 mg/mL branched polyethylene imine (BPEI) and 3 mg/mL poly(sodium 4-styrene sulfonate) (PSS) solutions of DI water at pH 6.5. Precursor layers were deposited by firstly immersing the wafers into BPEI solution for 30 min and rinsing solution for 2 min, secondly PSS solution for 30 min and rinsing solution for 2 min and this process was continued for 5 layers by deposition of precursor polymers alternately. After precursor layers were coated, multilayers were prepared by self-assembly of PSS and PDMA-*b*-PDEA micelle solutions at the surface. The upmost layer of the precursor stack was BPEI, a positively charged polymer, thus,

LbL deposition of multilayers started with PSS. Concentration of PSS was 0.2 mg/mL and the concentration of PDMA-*b*-PDEA micelle solution was 1 mg/mL. PSS solution and rinsing solutions were prepared using 0.01 M Na<sub>2</sub>HPO<sub>4</sub> buffer. PDMA-*b*-PDEA solution was prepared using 0.01 M NaH<sub>2</sub>PO<sub>4</sub> buffer. Deposition pH values were either pH 8 or pH 8.5 for both PDMA-*b*-PDEA micelles and PSS. Deposition temperature was either 25°C or 30°C for both PDMA-*b*-PDEA micelles and PSS. Deposition time was 5 minutes for each polymer in all experiments. Multilayer growth and pH-stability were followed using ellipsometry by measuring the dry film thickness.

## **2.6 pH-Stability of the Multilayers**

Multilayers were immersed into 0.01 M phosphate buffered saline (PBS) solutions (1 tablet dissolved in 200 mL DI water) for 30 minutes at different pH values and at different temperatures (25°C, 37.5°C) to investigate the pH stability. After 30 min exposition to pH adjusted PBS solutions, dried film thicknesses were measured with ellipsometer. Long-term pH stability of multilayers were also examined by immersing the films into PBS solutions at pH6, at 25°C and 37.5°C for 8.5 hours in order to support pyrene release experiments of multilayers. Figures of pH-stability of multilayers are given as fraction retained at the surface as a function of pH. To calculate the fraction retained at the surface at each pH, film thickness is divided by the initial thickness of the film.

## **2.7 Release of Pyrene from Multilayers**

PSS and pyrene loaded PDMA-*b*-PDEA micelles were deposited as 30 bilayers on both sides of a glass slides at pH 8, 25°C. Multilayers were immersed into PBS solution at pH 6 and for control group at pH 8 at 25°C, 37.5°C. Release of pyrene is followed by taking samples for every 30 minutes from the PBS solution in which multilayers exposed to. Fluorescence intensity of this samples were measured as function of time. Excitation wavelength was arranged to 335 nm and the intensity at 375 nm (emission wavelength of pyrene) was monitored. Pyrene release experiment was continued until the intensity at 375 nm is stabilized.



## CHAPTER 3

### RESULTS AND DISCUSSION

#### 3.1 pH-Induced Micellization of PDMA-*b*-PDEA

PDMA-*b*-PDEA copolymer is soluble in acidic medium when both blocks are protonated.  $pK_a$  values of PDMA and PDEA homopolymers are 7.0 and 7.3, respectively [23]. The amino groups on both blocks unprotonate as the pH is increased. However, there is a distinct difference in the behavior of these two polymers at pH above their  $pK_a$  values. Above pH 7.3, PDEA becomes water-insoluble and phase separates in the solution [46]. In contrast, PDMA remains soluble in water even above its  $pK_a$  [83]. The difference in the behavior of these two polymers can be explained by greater hydrophobicity of PDEA than that of PDMA due to two additional methylene groups of PDEA. By taking advantage of the difference in the solubility of these two blocks, micellization could be induced via pH trigger. Above pH 7.5, PDMA-*b*-PDEA formed micellar aggregates with PDEA-core and PDMA-corona structure. Micellization of PDMA-*b*-PDEA was followed by measuring the hydrodynamic size as a function of pH using dynamic light scattering technique (Figure 8). PDMA-*b*-PDEA existed as unimers at acidic conditions. Hydrodynamic size of PDMA-*b*-PDEA sharply increased above pH 7. PDMA-*b*-PDEA micelles (BCMs) with 25 nm were obtained above pH 7.5. The driving force for the micellization is the enhanced hydrophobic-hydrophobic interactions among the PDEA blocks above its  $pK_a$ . PDMA which is soluble above its  $pK_a$  assures the stability of PDMA-*b*-PDEA micelles in aqueous solution.

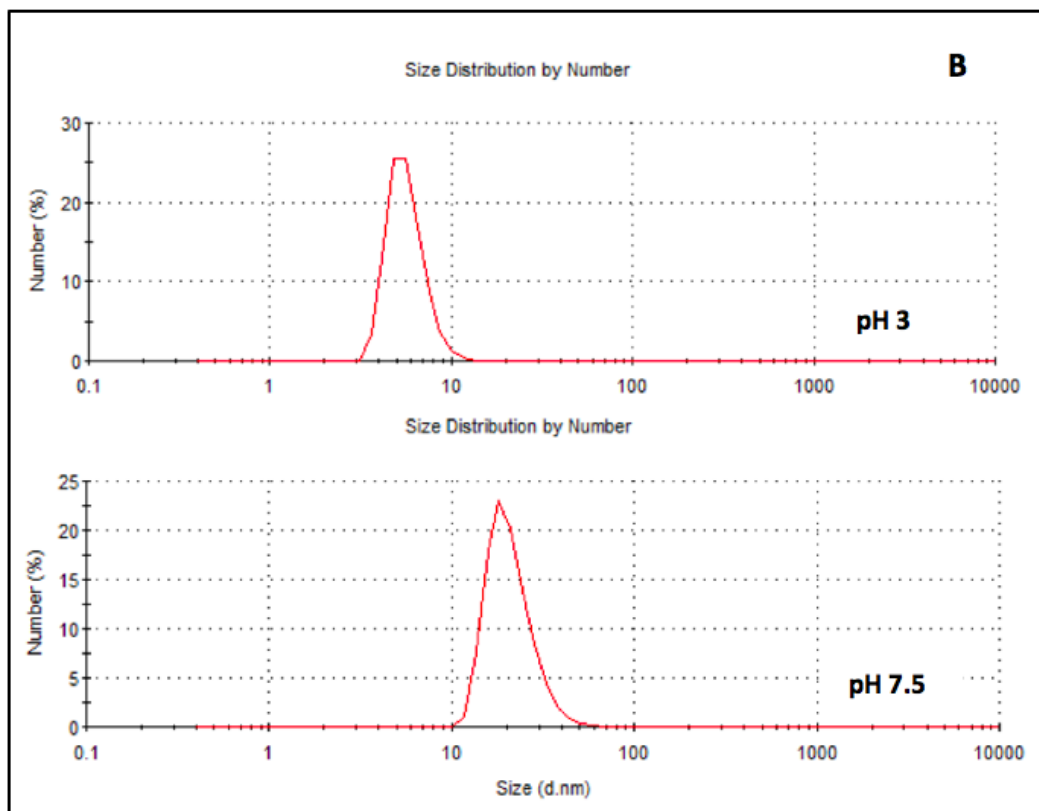
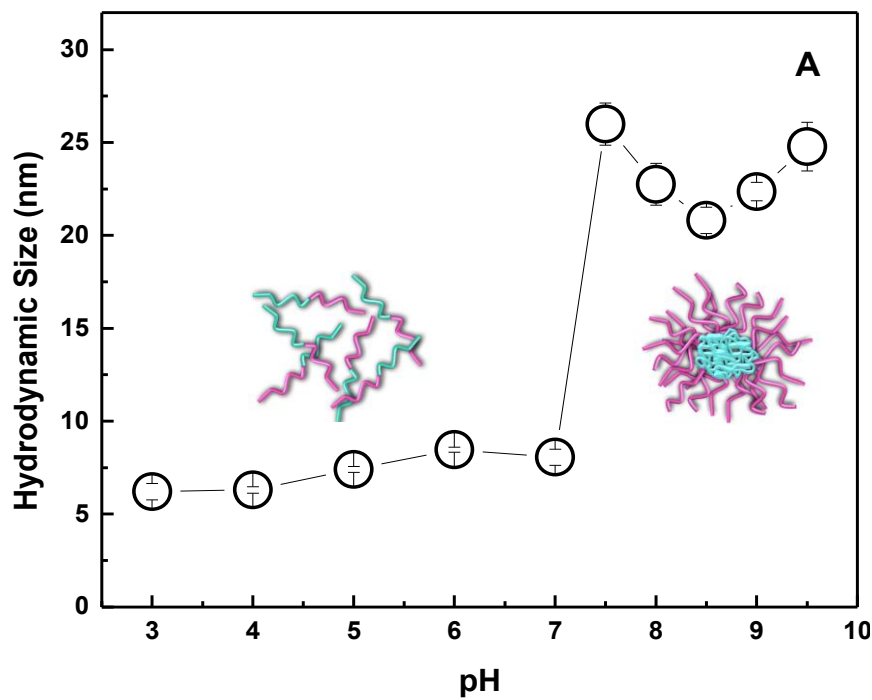


**Figure 8.** Hydrodynamic size as a function of pH (Panel A); size distribution curves of PDMA-*b*-PDEA at 25°C, at pH 3 and pH 7.5 (Panel B).

Zeta potential of PDMA-*b*-PDEA was also examined as a function of pH (Fig. 9). The positive zeta potential decreased as the pH increased due to deprotonation of the amino groups on PDMA and PDEA blocks. At pH 9, PDMA-*b*-PDEA micelles were almost electrically neutral. Further increasing pH resulted in negative zeta potential probably due to buffer anions adsorbed on the micellar corona.

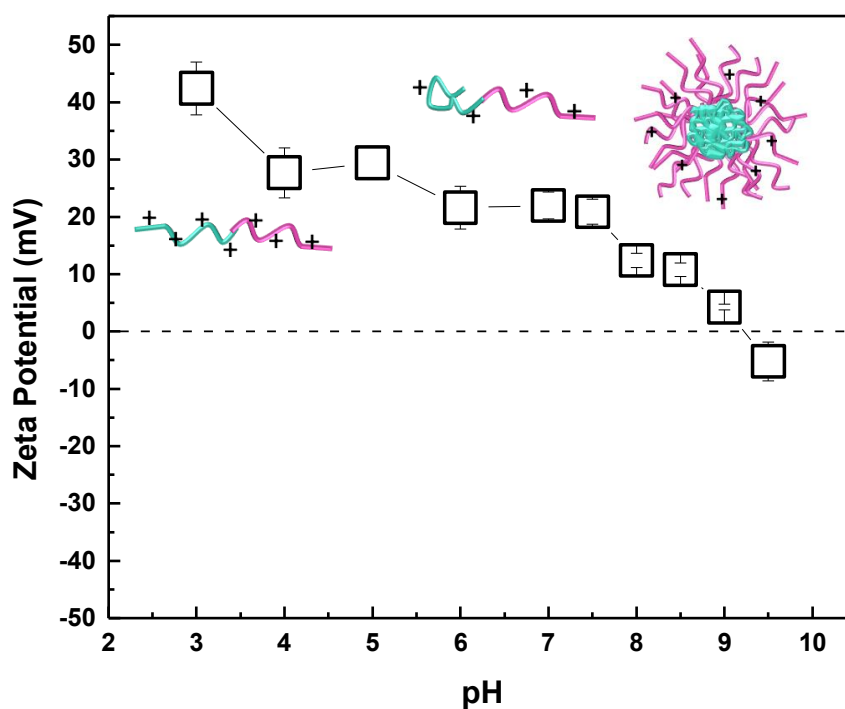


**Figure 9.** Zeta potential of PDMA-*b*-PDEA as a function of pH.

In addition to hydrodynamic size and zeta potential measurements, TEM image was taken. To take TEM image, a drop of PDMA-*b*-PDEA micelle solution at pH 8 was placed on the surface of a copper grid coated with a carbon substrate then surface was air dried. As seen in figure 10, TEM image also confirms formation of micelle structures above pH > 7.5.

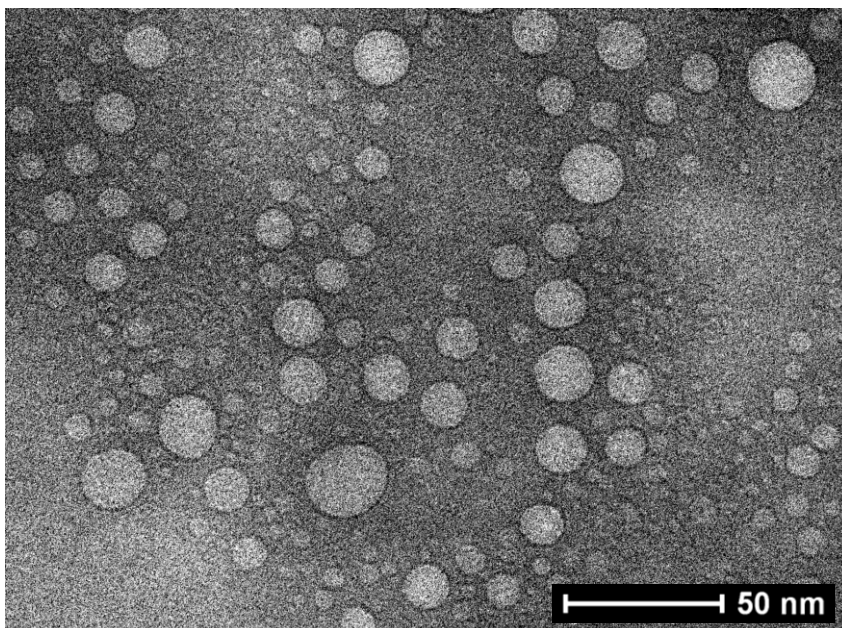


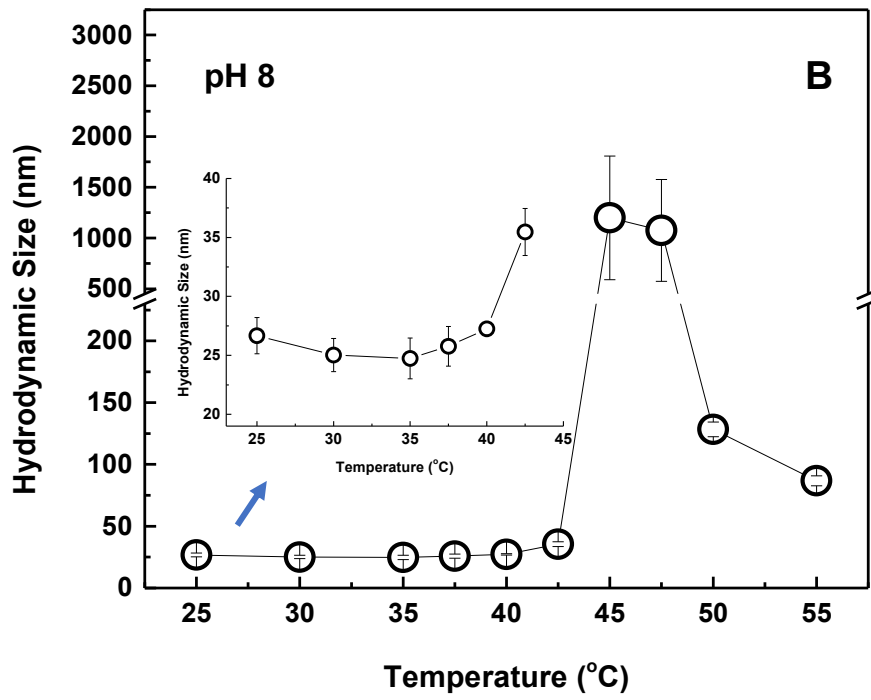
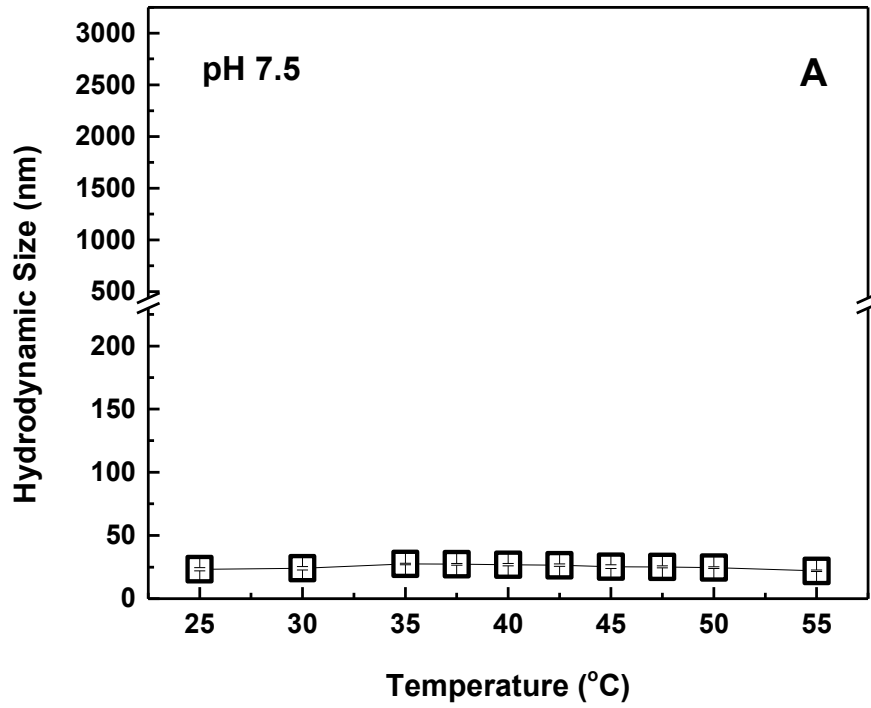
**Figure 10.** TEM image of 1mg/ml PDMA-*b*-PDEA micelle solution at pH 8, 25°C.

### 3.2 pH-Dependent Thermo-Responsive Behavior of PDMA-*b*-PDEA Micelles

Thermo-responsive behavior of PDMA-*b*-PDEA micelles was examined at pH 7.5, pH 8 and pH 8.5. PDMA has a LCST of 40-50 °C [90]. PDMA is a weak polyelectrolyte, therefore the pH of the PDMA solution was expected to affect the critical phase transition temperature of PDMA. It is known that pH affects LCST-type behavior of PDMA [91,92]. The hydrodynamic size of PDMA-*b*-PDEA micelles was followed as a function of temperature by either 2.5°C or 5°C increase at each step to understand the effect of charge density of PDMA on the LCST-type phase behavior of PDMA and the aqueous pH-stability of PDMA-*b*-PDEA micelles. As seen in Figure 11, no significant change in hydrodynamic size was detected between 25-55°C at pH 7.5 . In contrast, the hydrodynamic sizes increased abruptly above a certain temperature at pH 8 and pH 8.5. For example, at pH 8, a slight increase in hydrodynamic size was detected at 37.5 °C. The size gradually increased up to 42.5°C. Beyond 42.5°C, a dramatic increase in particle size was monitored, followed by precipitation of PDMA-*b*-PDEA micelles with time. At pH 8.5, the first slight increase was observed at 35 °C. The particle size increased gradually up to 40°C. The sharp increase in size was detected at 42.5°C, followed by precipitation of PDMA-*b*-PDEA micelles with time. The decrease in the critical temperature with



increasing pH of PDMA solution can be correlated with the charge density of the PDMA-coronal chains. In general, polymers with LCST form hydrogen bonds with the water molecules surrounding them. As the temperature rises, the hydrogen bonds among the polymer chains and water molecules are disrupted and the polymer-polymer interactions are enhanced. The polymer goes into a conformational transition from extended to globular coil as the temperature approaches the critical value [93]. In case of PDMA-*b*-PDEA micelles, PDMA-coronae is partially positively charged at pH 7.5. The intra-molecular electrostatic repulsion among the like charges prevents a conformational transition from extended to globular coil and also reduces the polymer-polymer interactions. As Fournier et al. explained at low pH, polymer do not show LCST due to high hydrophilicity of PDMA since most amino groups are protonated [94]. Of note, it is worth to mention that ion-dipole interactions among the protonated amino groups and water molecules are relatively stronger than the hydrogen bonding interactions among the unprotonated amino groups and water molecules. Thus, it is more difficult to disrupt the ion-dipole interactions than to disrupt the hydrogen bonding interactions with increasing temperature. Therefore, the greater hydrophilicity of PDMA at pH 7.5 was another reason that a temperature response was not observed. Similar to our findings Yuk et al. also could not observe an LCST behavior of PDMA in a situation where the polymer was protonated at low pH [95]. As mentioned above, PDMA-*b*-PDEA micelles demonstrated temperature-responsive behaviors at pH 8 and pH 8.5 due to decrease in the charge density on PDMA-coronae. The lower charge density resulted in lower electrostatic repulsion among the PDMA chains which could no longer prevent the conformational transition. Besides, the hydrophilicity of PDMA chains decreased as the pH was increased resulting in enhanced polymer-polymer interactions.



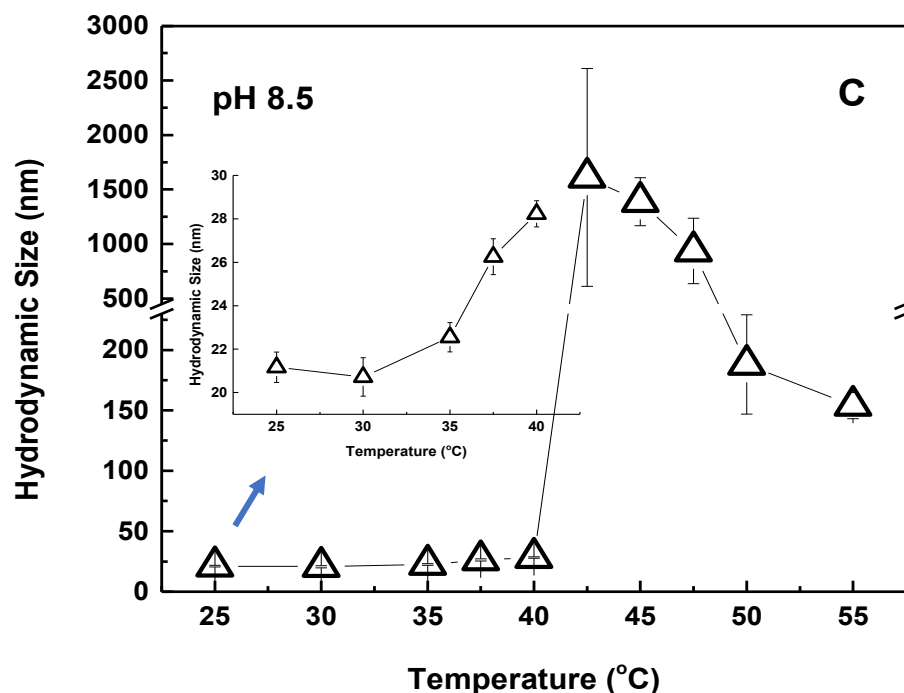


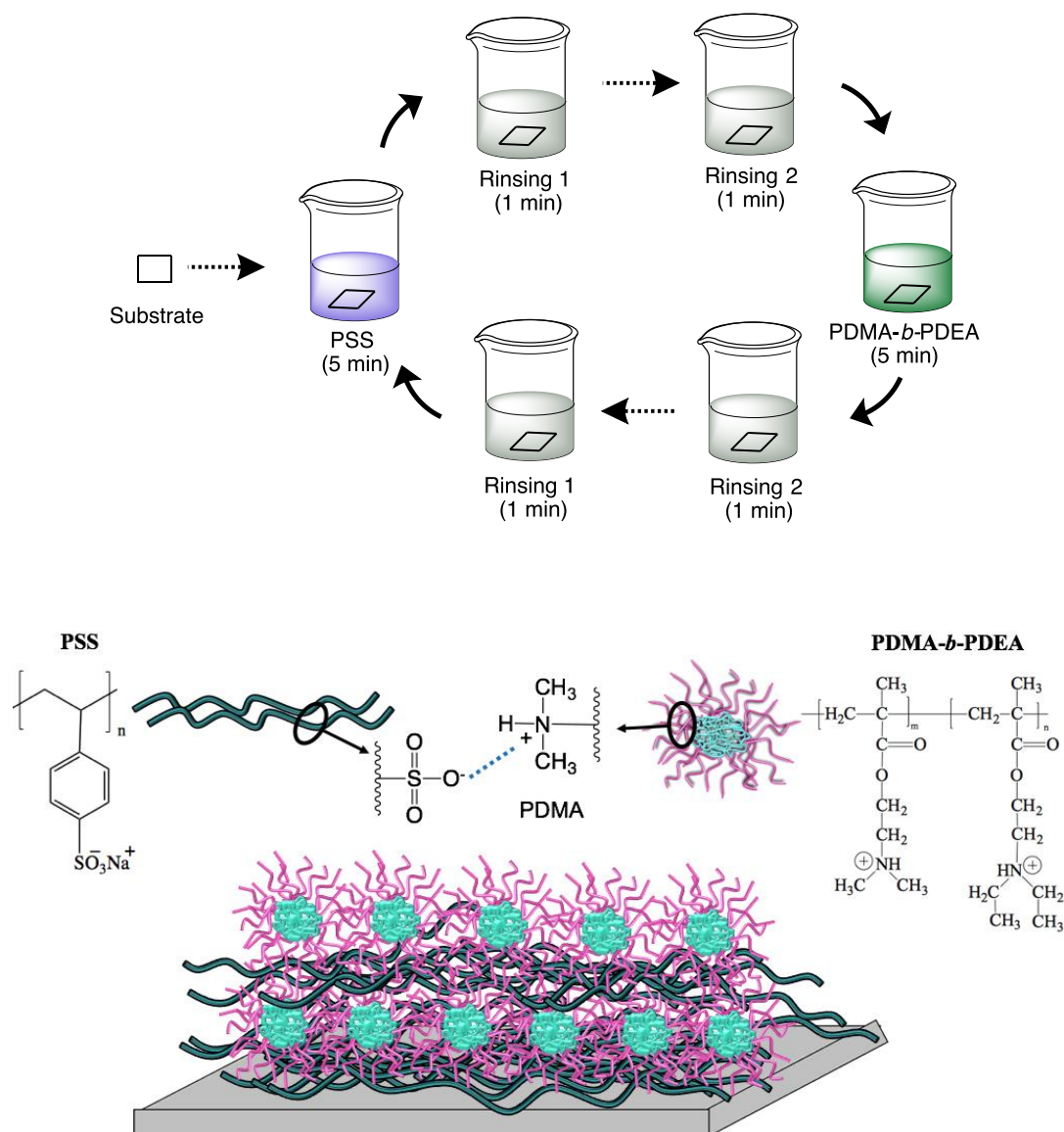
**Figure 11.** Hydrodynamic size of PDMA-*b*-PDEA micelles as a function of temperature and the size distributions of PDMA-*b*-PDEA micelles by number with increasing temperature at pH 7.5 (A), pH 8 (B), pH 8.5 (C).

### 3.3 Multilayers of PSS and PDMA-*b*-PDEA micelles

The number of studies concerning films of PDMA-*b*-PDEA micelles is limited. These studies were reported on i) the effect of concentration and chain length on the pH-response of a monolayer of PDMA-*b*-PDEA micelles [84], ii) the adsorption kinetics of PDMA-*b*-PDEA micelles on silica/aqueous solution interface [85], iii) deposition of multilayers of nonquaternized or quaternized PDMA-*b*-PDEA micelles coated on polystyrene latex [88] and silica nanoparticles [86,87], and iv) pH-induced reversible uptake and release of pyrene from a monolayer of PDMA-*b*-PDEA micelles adsorbed onto silica particles [89]. Different from these studies, in this study, the effects of deposition pH and deposition temperature on the multilayer thickness and post-assembly behavior of the films have been investigated in detail.

### 3.3.1 Effect of Deposition pH on LbL Growth

Multilayers of PSS and PDMA-*b*-PDEA micelles were constructed at pH 8 and pH 8.5 via LbL technique as seen in scheme 3. The driving force for multilayer growth was the electrostatic interactions between the negatively charged sulfonate ( $\text{SO}_3^-$ ) groups of PSS and positively charged protonated tertiary amino ( $\text{R}_3\text{NH}^+$ ) groups of PDMA-coronae.



**Scheme 3.** LbL film preparation process of PSS and PDMA-*b*-PDEA micelles

Figure 12 shows the LbL growth of PDMA-*b*-PDEA micelles/PSS films at pH 8 and pH 8.5. PDMA-*b*-PDEA micelles/PSS films demonstrated a linear growth profile at pH 8. However, multilayer growth at pH 8.5 was not linear and the thickness increment upon PSS deposition was lower when compared to the PDMA-*b*-PDEA micellar layer. PSS is a strong polyelectrolyte and is highly charged at pH 8.5. Unlike PSS, PDMA-corona is slightly charged at the same conditions. The interpolyelectrolyte complexes formed among the PDMA-*b*-PDEA micelles and PSS at the surface are expected to be highly hydrophilic due to excess negative charge on the PSS chains. This results in the solubilization of some amount of PDMA-*b*-PDEA micelles from the surface.

As seen in the figure 12, only 0.5 pH unit increase in the BCM solution resulted in a significant increase in film thickness. This difference can be correlated with the difference in the charge density at pH 8 and pH 8.5. The greater charge density at pH 8 results in i) more extended conformation of PDMA and ii) greater number of binding points among the PDMA-*b*-PDEA micellar and PSS layers. Both effects led to thinner but more intense films at pH 8. At pH 8.5, PDMA-corona adopts more globular conformation. In addition, the lower charge density on PDMA results in lower number of binding points among the layers. These effects led to thicker, but more loose films at pH 8.5. Scheme 4 demonstrates the difference in the multilayer structure at pH 8 and pH 8.5.

Our results are in good agreement with the studies of other groups which investigated the effect of pH on the growth of multilayers. Peterson and co-workers also examined the pH effect on PEM coatings of poly-L-histidine (PLH) and poly(methacrylic acid) (PMAA) [96]. According to study, assembly pH impacts the amount of polyelectrolyte adsorbed therefore PEMs with the same number of bilayers assembled at different pH values have different mass and thickness. According to their interpretation, as assembly pH leads to more charge density on polyelectrolytes, layer entanglement behavior due to attraction of opposite charges of polyelectrolytes dominates the structure of PEM resulting more compact multilayers.

Additionally, Grunze and co-workers showed that multilayers grow linearly at pH 7.2. In contrast, they observed a nonlinear increase in mass and thickness when the multilayers are prepared at PEI pH 8.0/PAA pH 5.0 and as pH difference increases

nonlinearity increases also [97]. According to them, the films constructed in the latter situation enhances the concentration of uncompensated polycations/polyanions within the multilayer, which increases the growth per each coating cycle.

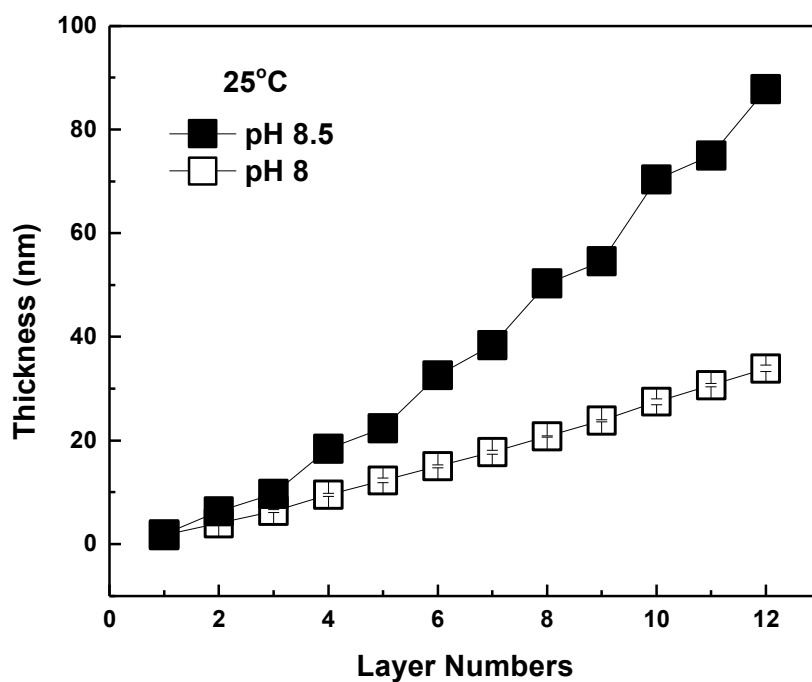
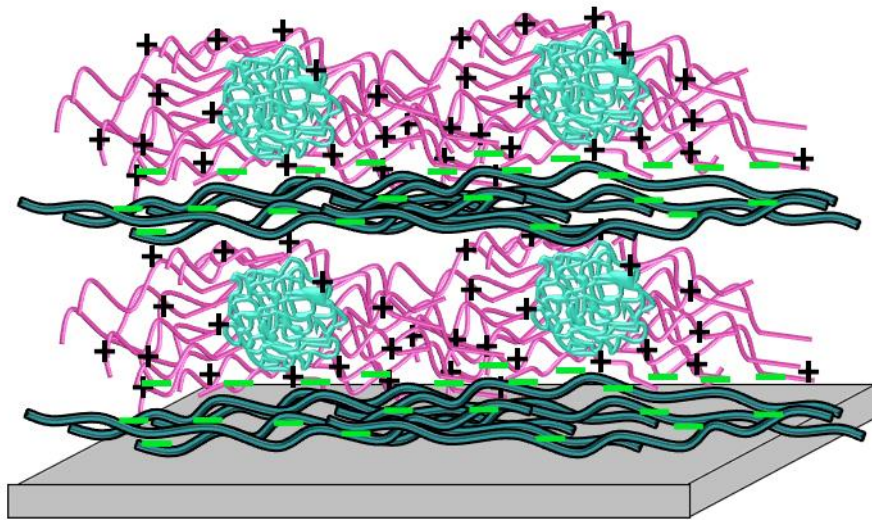
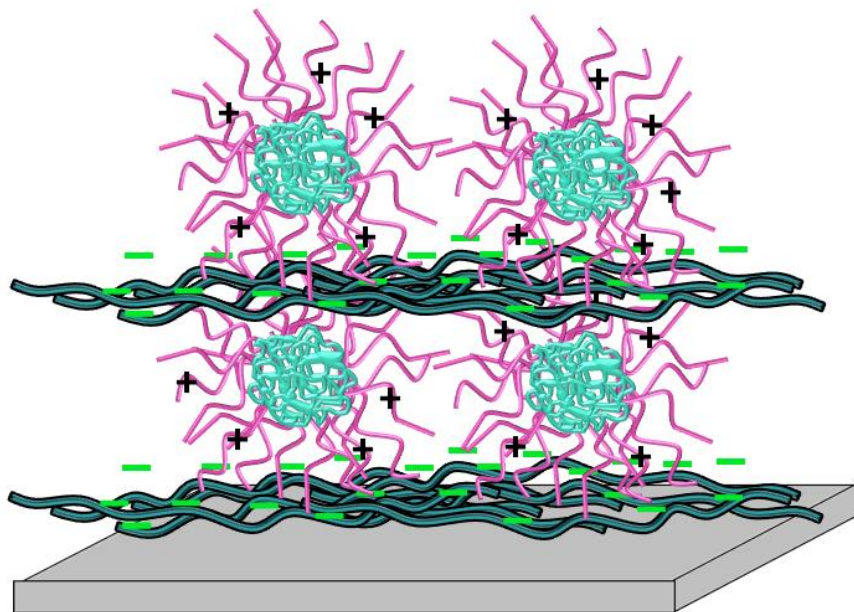


**Figure 12.** Effect of deposition pH on the multilayer growth of PSS and PDMA-*b*-PDEA micelles at 25°C.



pH 8



pH 8.5

**Scheme 4.** Schematic representation of multilayers deposited at pH 8 and pH 8.5

### 3.3.2 Effect of Deposition Temperature on LbL Growth

The effect of temperature-sensitive phase behavior of PDMA on the multilayer growth was examined. Multilayers were constructed at 30°C at pH 8 and pH 8.5 and the results are contrasted with the thickness data obtained at 25°C (Figure 13). The thickness of the multilayers constructed at 30°C was higher than that obtained at 25°C at both pH values. The higher film thickness at 30°C can be correlated with the LCST-type phase behaviour of PDMA. PDMA adopts globular coil conformation as the temperature approaches its critical value. Therefore, PDMA is expected to adopt more extended coil conformation at 25°C compared to its conformation at 30°C. This conformational difference led to higher thickness values at 30°C than that obtained at 25°C. Scheme 5 demonstrates the differences in the conformation of PDMA coronal chains as well as the multilayer structure at 25°C and 30°C.



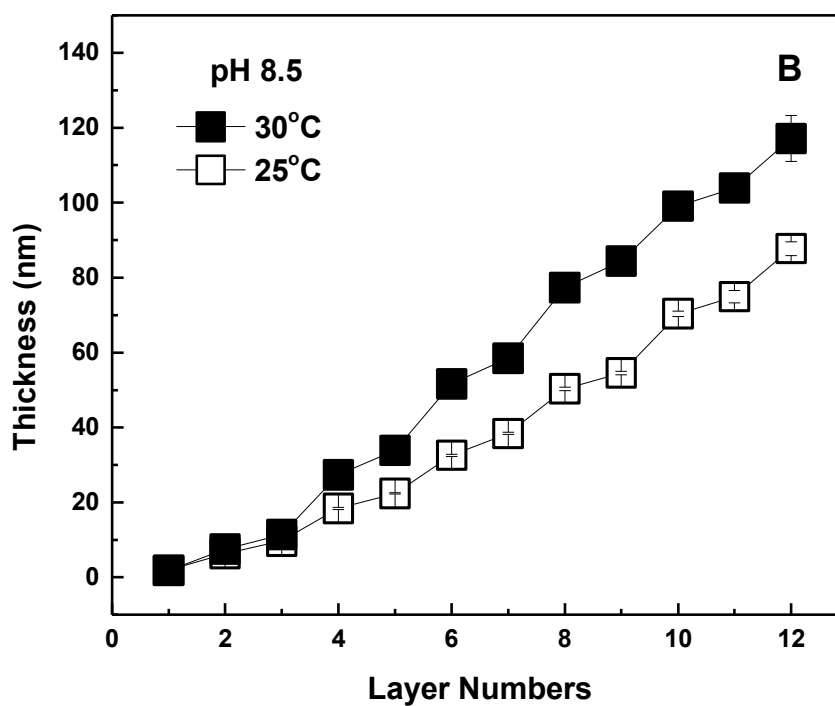
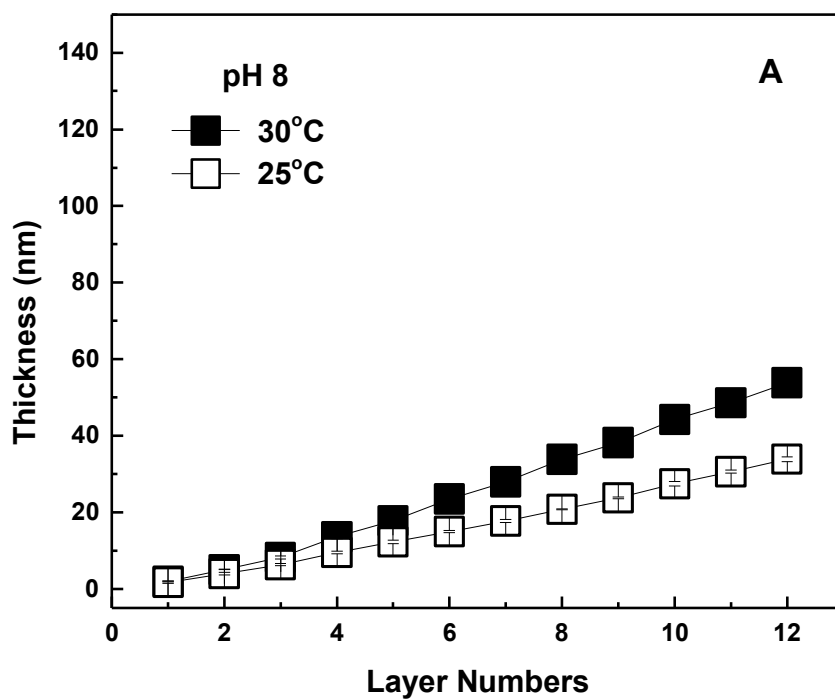
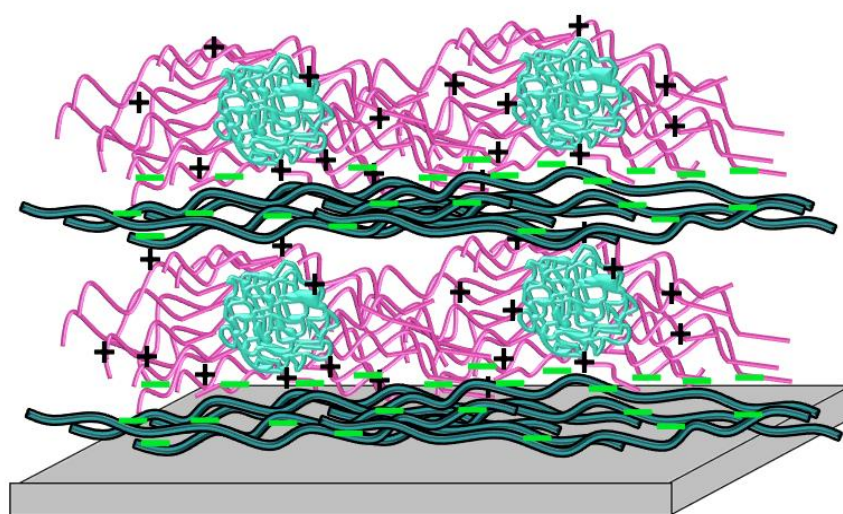
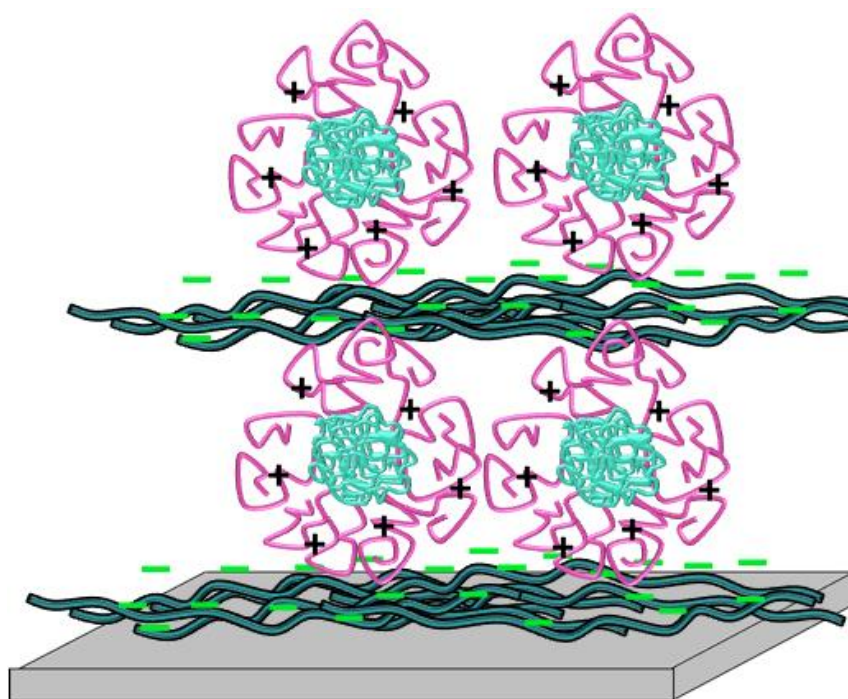


**Figure 13.** Multilayer growth at 30°C at pH 8 (Panel A) and pH 8.5 (Panel B). The data obtained at 25°C is plotted for comparison.



25 °C



30 °C

**Scheme 5.** Schematic representation of multilayers deposited at 25°C and 30°C.

Importantly, the difference in the thickness of the films at pH 8 and pH 8.5 increased at 30°C. This can be explained by the lower charge density on the PDMA-corona at

pH 8.5 which enabled PDMA to adopt more globular coil conformation due to lower intra-molecular electrostatic repulsion when compared to PDMA at pH 8. Figure 14 clearly contrasts the thickness values for a 12-layer PDMA-*b*-PDEA micelles/PSS films, deposited at i) 25°C, pH 8 and pH 8.5 and ii) 30°C, pH 8 and pH 8.5.

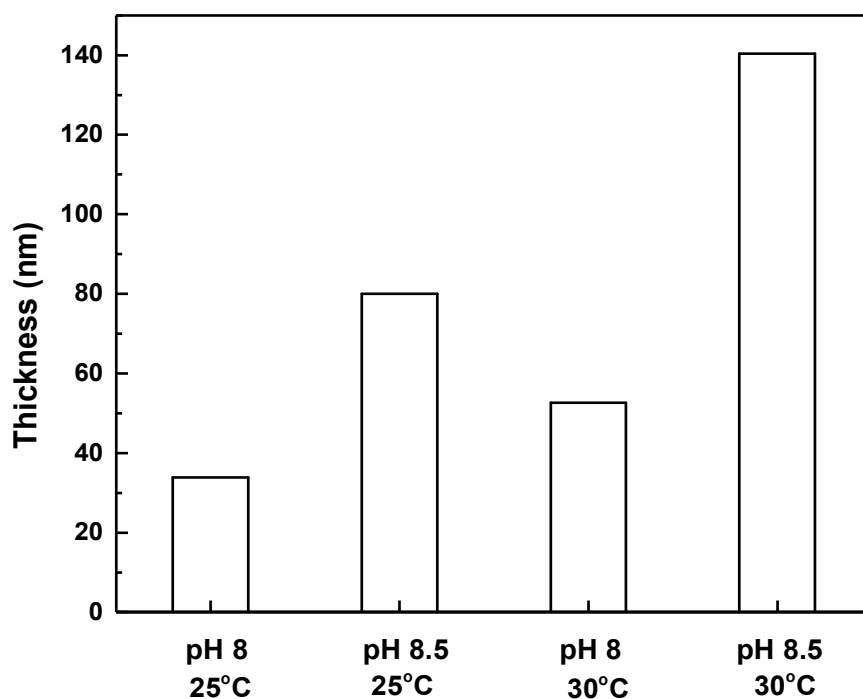


**Figure 14.** Comparison of the thickness of a 12-layer PDMA-*b*-PDEA micelles/PSS deposited under different pH and temperature conditions.

It was previously reported that multilayers of polymers showing LCST-type phase behavior (e.g. PNIPAM), gave higher film thickness at temperatures near to or above the LCST value [70]. This study is the first demonstrating the effect of pH-dependent thermo-responsive behavior of PDMA on the LbL growth of PDMA-*b*-PDEA micelles/PSS films.

### 3.4 pH-Stability of Multilayers of PDMA-*b*-PDEA Micelles and PSS

In this part of the study, multilayers were exposed to PBS solutions of decreasing pH at 25°C and 37.5°C. The reason to use PBS was to mimic the biological environment. The effects of deposition pH and the deposition temperature on the stability of the multilayers are discussed.

#### 3.4.1 Effect of Film Deposition pH on the pH-Stability of Multilayers

Multilayers which were constructed at pH 8 (at 25°C) and pH 8.5 (at 25°C) were exposed to PBS solutions of decreasing pH at 25°C for 30 minutes at each pH value. Figure 15 shows the fraction retained at the surface at moderately acidic and strongly acidic environment for the multilayers constructed at pH 8 and pH 8.5, respectively. Multilayers, which were constructed at pH 8 and exposed to PBS solution of decreasing pH were quite stable at the acidic region at 25°C. ~85% of the film remained at the surface even at strongly acidic conditions. In contrast, multilayers which were constructed at pH 8.5 (at 25°C) were quite unstable when exposed to PBS solutions of decreasing pH at 25°C. Multilayers were removed completely from the surface at pH 7.5. Note that, pH 7.5 is the critical micellization pH for PDMA-*b*-PDEA, therefore PDMA-*b*-PDEA exist as both unimers and micelles in the solution. The disintegration of the multilayers can be correlated with the protonation of both blocks of PDMA-*b*-PDEA which resulted in a charge imbalance within the multilayers and partial removal of the polymers from the surface. Disintegration of multilayers due to charge imbalance and increase in osmotic pressure has been earlier reported by Schlenoff and Sukhorukov [98,99].

Scheme 6 shows micelle disintegration and film disintegration for multilayers constructed at pH 8 and pH 8.5. The difference in the disintegration profiles of the films is due to the strength of binding among the layers. Multilayers which were constructed at pH 8.5 had low number of binding points among the layers, thus the stability of the films for the charge imbalance created within the multilayers with decreasing pH was low. In case of multilayers which were constructed at pH 8, although PDMA-*b*-PDEA micelles disintegrate below the critical micellization pH of 7.5, significant amount of the multilayers remained at the surface even at strongly

acidic conditions. This suggests a restructuring among PDMA-*b*-PDEA unimers and PSS via electrostatic interactions among the negatively charged PSS and positively charged PDMA or PDEA within the multilayers. In Section 3.6.2, the disintegration of the PDMA-*b*-PDEA micelles will be confirmed by the release of pyrene at acidic conditions.

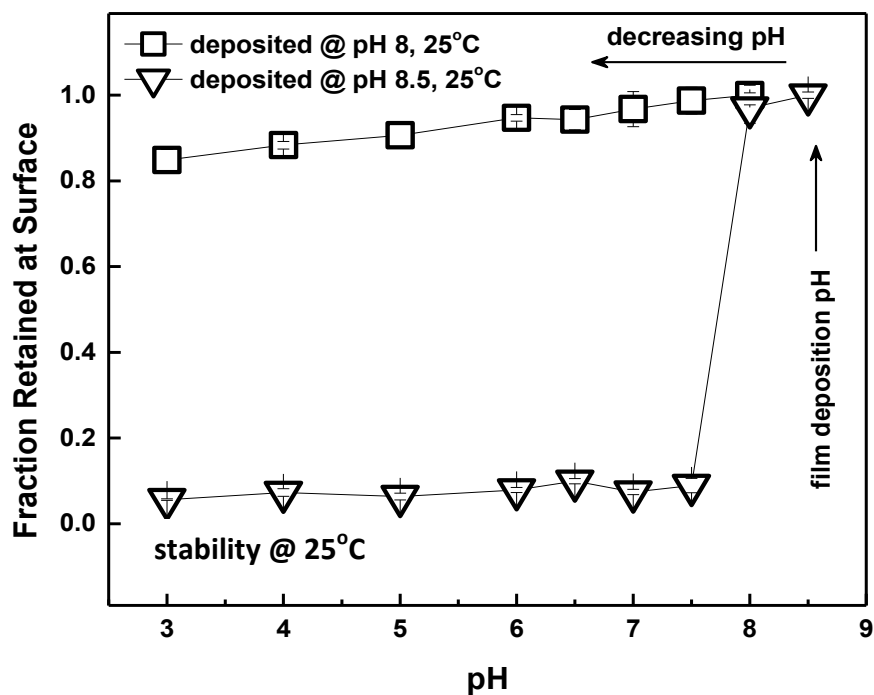
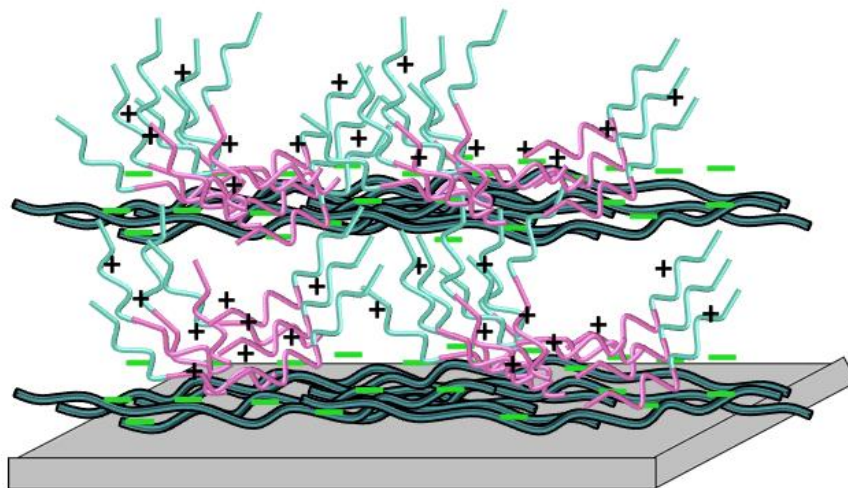
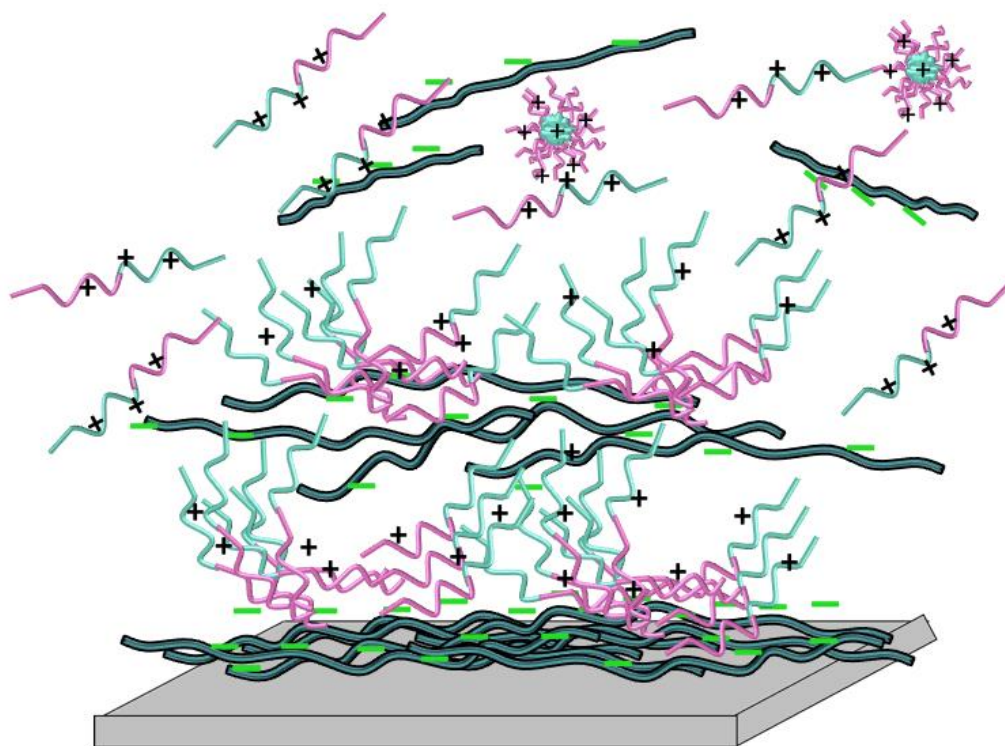


**Figure 15.** Fraction retained at the surface after exposure to PBS solutions of decreasing pH at 25°C for multilayers constructed at pH 8 or pH 8.5, at 25°C.



**pH 8 film, micelle disintegration at pH 6**

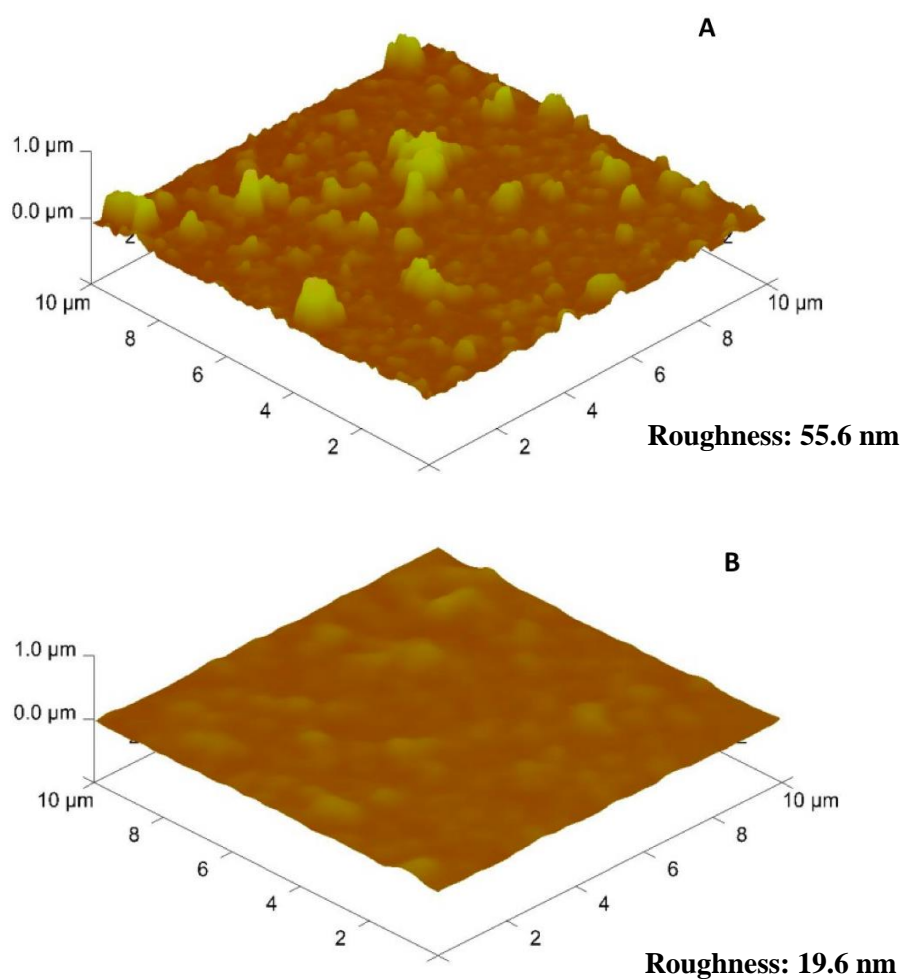


**pH 8.5 film, film disintegration at pH 7.5**

**Scheme 6.** Schematic representation of micelle disintegration and film disintegration for multilayers constructed at pH 8 and pH 8.5.

Figure 16, comparison between AFM images of 20 bilayer PSS/ PDMA-*b*-PDEA film deposited at pH 8, 25°C and same film after immersion into PBS solution at pH

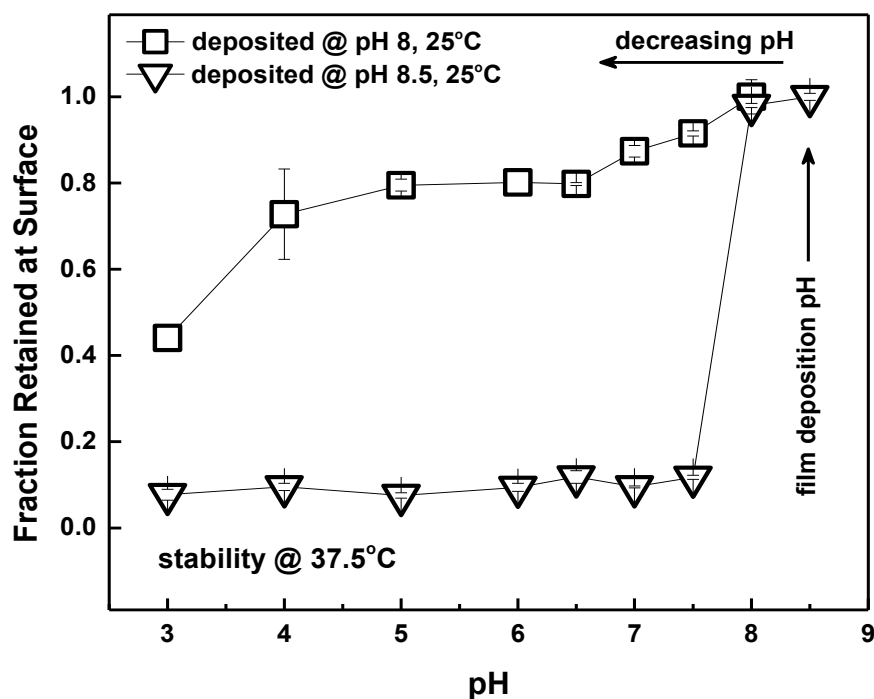
6, 25°C clearly verifies the disintegration of the micelles within the multilayers at pH 6. The roughness of the film decreased after it was kept in PBS solution at pH 6, 25°C for 6 hours. Film roughness is decreased because micelles left their globular shape and spread on the surface due to disintegration of micelle core, PDEA, at pH 6.



**Figure 16.** AFM, topography images (10 μm x 10 μm) of 20 bilayer PSS/ PDMA-*b*-PDEA film deposited at pH 8, 25°C (Panel A) and film immersed into PBS solution at pH 6, 25°C for 6 hours (Panel B).

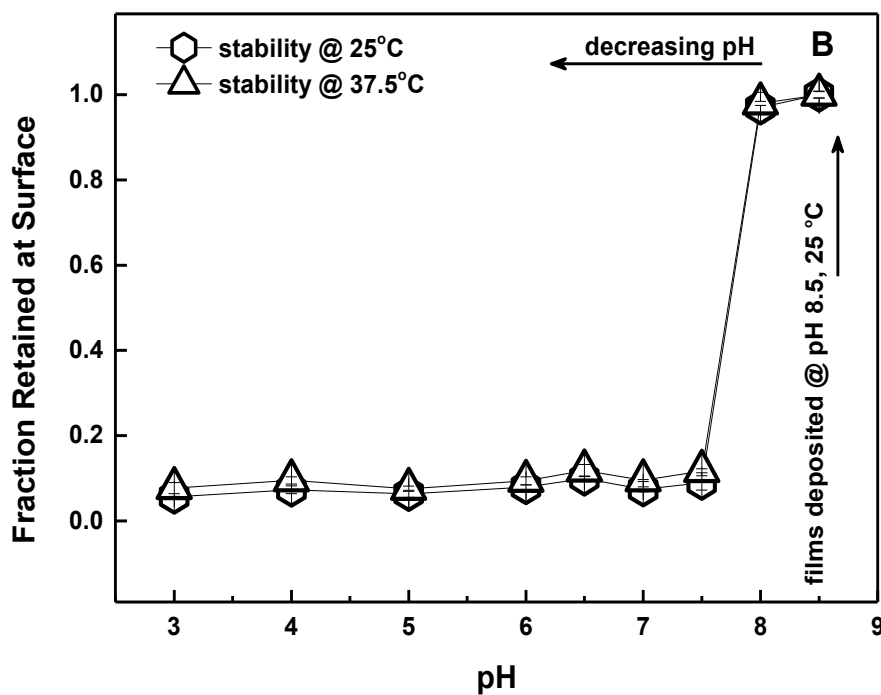
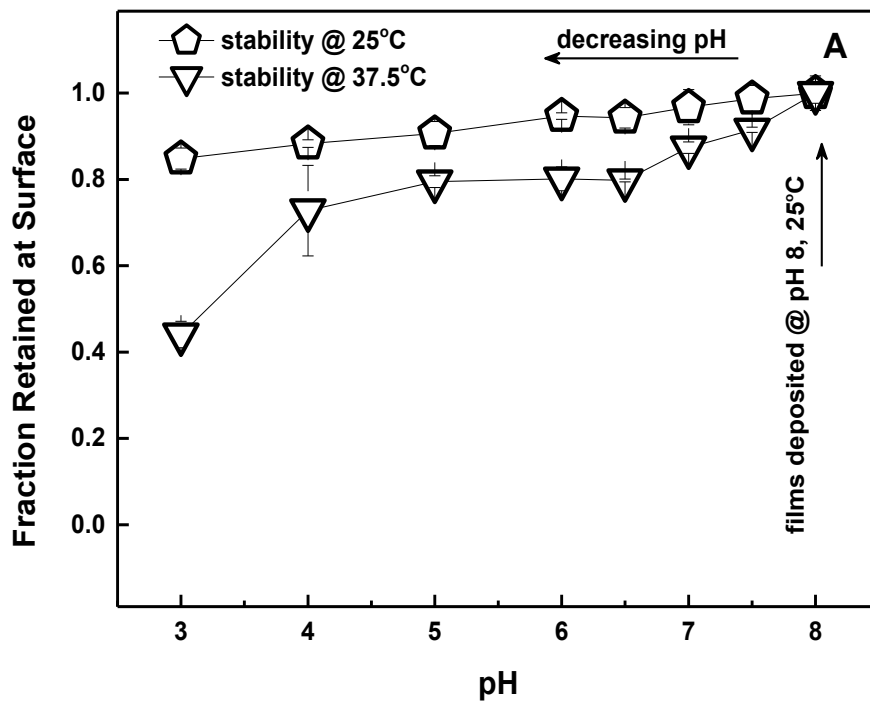
### 3.4.2 Effect of Post-Assembly Temperature on the pH-Stability of Multilayers

The pH-stability of the films which were constructed at pH 8 decreased significantly when exposed to PBS solutions of decreasing pH at 37.5°C (Fig. 17). Multilayers disintegrated gradually and more than 50 % of the film removed from the surface at strongly acidic conditions. Remember that multilayers which were constructed at pH 8 and exposed to PBS at 25°C were quite stable in the acidic region. The decrease in thickness of PDMA-*b*-PDEA micelles/PSS films can be due to the disruption of the electrostatic interactions among the layers with the rising temperature. The pH-stability profiles of the multilayers which were constructed at pH 8.5 were almost same at 25°C and 37.5°C (fig. 18B). Multilayers completely removed from the surface at pH 7.5 and 37.5°C.



**Figure 17.** Fraction retained at the surface after exposure to PBS solutions of decreasing pH at 37.5°C for multilayers constructed at pH 8 or pH 8.5, at 25°C.

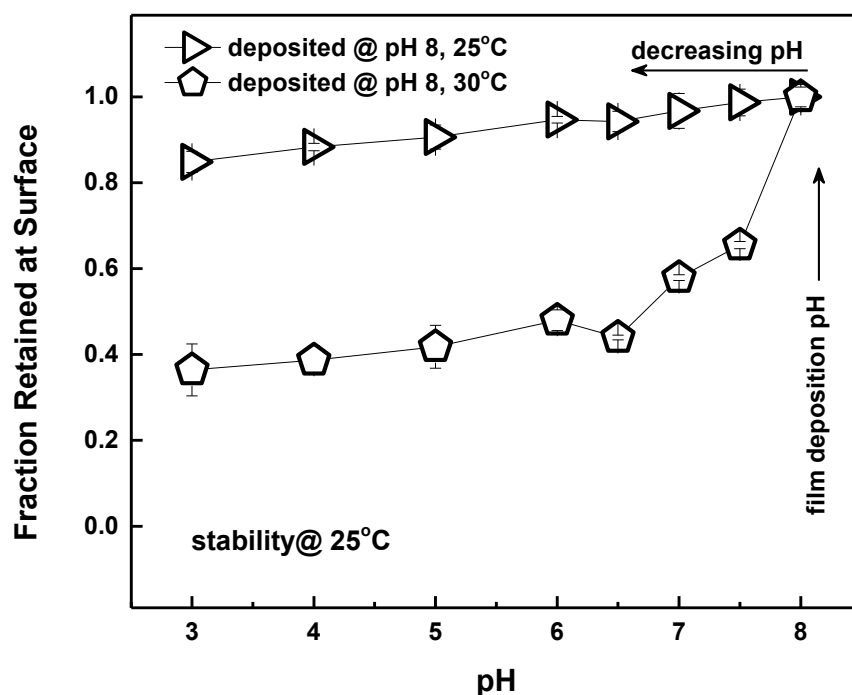




**Figure 18.** Fraction retained at surface after exposure to PBS solutions of decreasing pH at 25°C and 37.5°C for multilayers constructed at pH 8 (Panel A) and pH 8.5 (Panel B) at 25°C

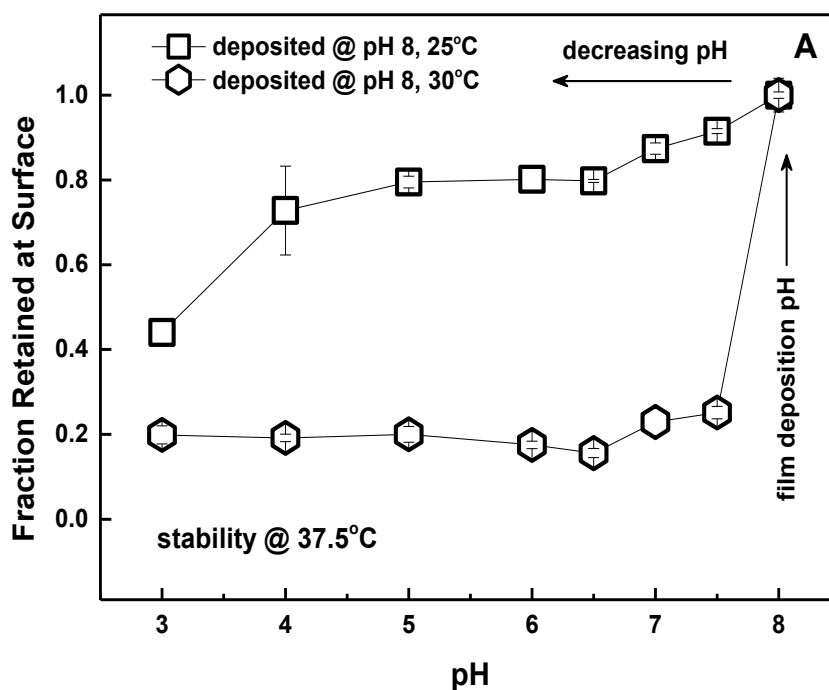
### 3.4.3 Effect of Film Deposition Temperature on the pH-stability of Multilayers

First, multilayers which were prepared at pH 8, 30°C were exposed to PBS solutions of decreasing pH at 25°C. The data for the films which were prepared at pH 8, 25°C and exposed to similar conditions are plotted for comparison (Figure 19). In contrast to the stability of the multilayers which were constructed at 25°C, the multilayers which were built up at 30°C gradually disintegrated with decreasing pH. The difference in the stability of the multilayers can be correlated with the internal structure of the multilayers (Scheme 5, page 36). Multilayers which were constructed at 25°C when PDMA coronal blocks adopt extended coil conformation are more intense and strongly bound than the multilayers which were constructed at 30°C when PDMA coronal blocks adopt globular coil conformation. The difference in the binding strength among the layers play a critical role in the pH-stability of the multilayers at the acidic region. Multilayers which were constructed at 30°C gradually disintegrated as the acidity of the solution increased. The amount of the film retained at the surface at strongly acidic conditions was ~ 40% of the initial film.



**Figure 19.** Fraction retained at the surface when the multilayers constructed at pH 8, 25°C or pH 8, 30°C were exposed to PBS solutions of decreasing pH at 25°C.

Second, multilayers which were constructed at pH 8, 30°C were exposed to PBS solutions of decreasing pH at 37.5°C. The data for the films which were prepared at pH 8, 25°C and exposed to similar conditions are plotted for comparison (Figure 20A). The multilayers which were constructed at 30°C, released completely from the surface at pH 7.5, whereas ~ 90% of the films, which were constructed at 25 °C retained at the surface under the same conditions. Figure 20B contrasts the difference in the pH-stability profiles of the films constructed at 30 °C and exposed to PBS solutions with decreasing pH at 25 °C and 37.5 °C. As discussed in Section 3.4.2, the lower stability of the films at 37.5°C can be correlated with the disruption of electrostatic bonds among the layers with increasing temperature.



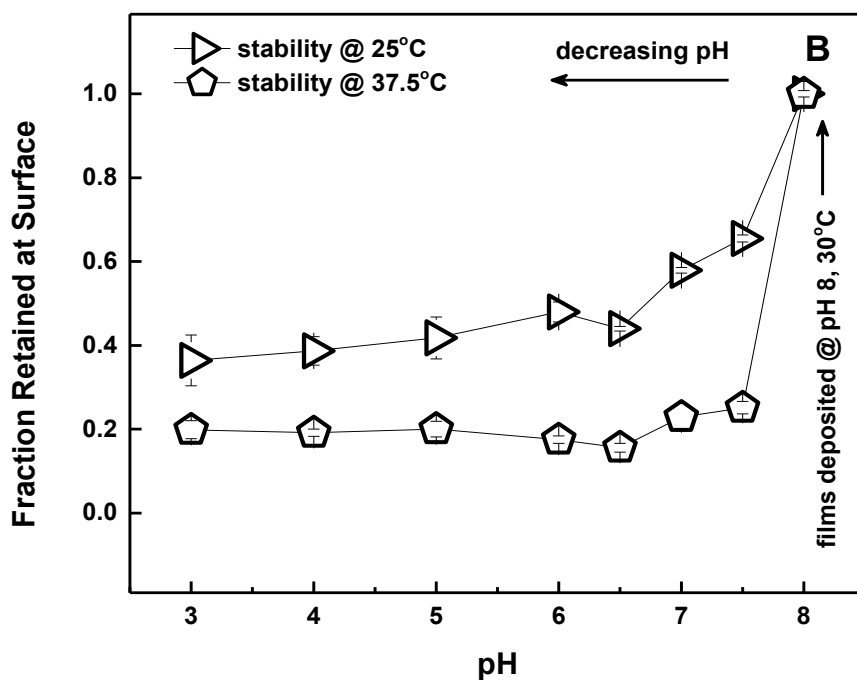


**Figure 20.** Fraction retained at the surface when the multilayers constructed at pH 8, 25°C or pH 8, 30°C were exposed to PBS solutions of decreasing pH at 37.5°C (Panel A). pH-stability profiles of the films constructed at 30 °C and exposed to PBS solutions with decreasing pH at 25 °C and 37.5 °C (Panel B).

### 3.5 Long-Term pH-Stability of the Multilayers

In this part of the study, the long-term pH-stability of the multilayers which were constructed at pH 8 and 25°C was examined at moderately acidic pH as a preliminary work for release studies which will be discussed in the next section. Remember that multilayers were previously exposed to different pH conditions only for 30 minutes. The reason to choose this film system was its greater stability at moderately acidic conditions than the multilayers constructed under different pH and temperature conditions, previously discussed in the previous sections in detail. As seen in Figure 21, no significant loss in film thickness was detected even after exposure to PBS solutions for 8.5 hours both at 25°C and 37.5 °C.

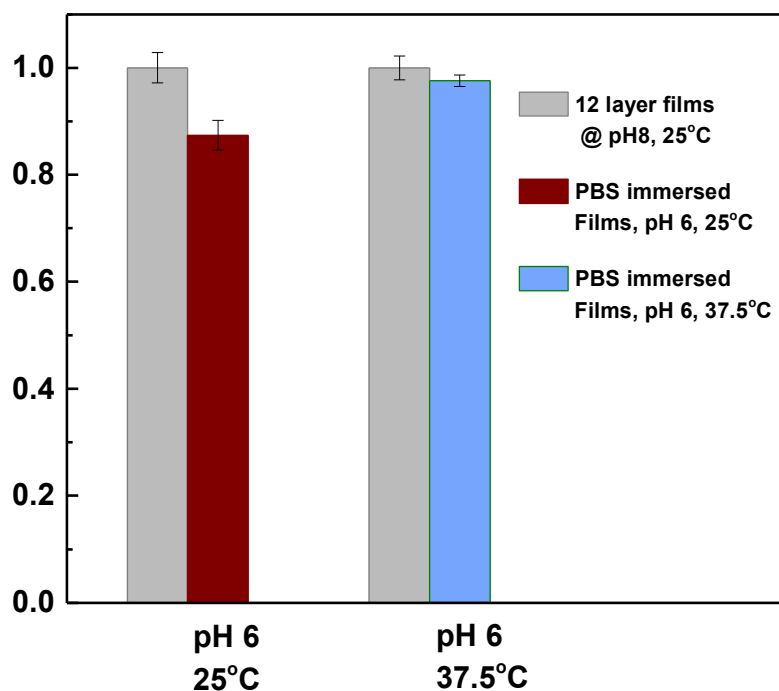
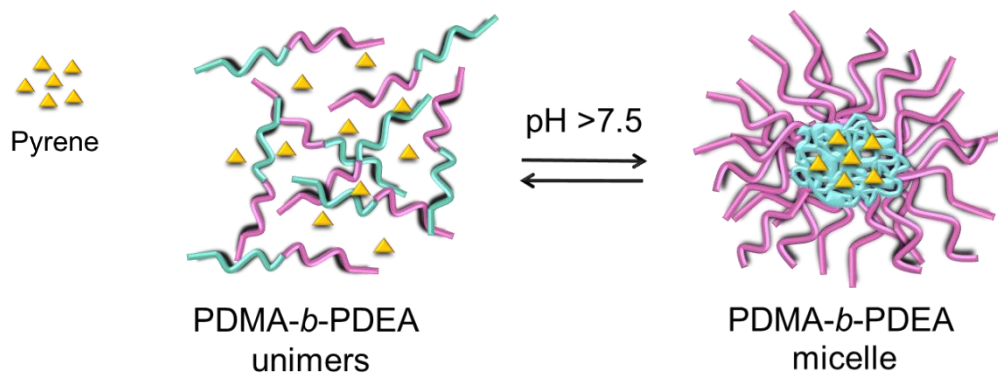


**Figure 21.** Fraction retained at the surface at pH 6 at 25°C and 37.5 °C after 8.5 hours. Grey columns represent the multilayers before immersion into PBS solution. Red and blue column represent the multilayers after immersion into PBS solution for 8.5 hours at pH 6, 25°C and pH6, 37.5°C respectively.

### 3.6 pH-Induced Release of Pyrene from the Multilayers

#### 3.6.1 Pyrene Loading into (PDMA-*b*-PDEA) Micelles

Pyrene was used as a model molecule to demonstrate the capability of the multilayers to release drug molecules at moderately acidic condition. Note that, multilayers which release drug molecules at moderately acidic conditions are of interest due to slightly acidic nature of the tumor cells. PDMA-*b*-PDEA was dissolved in  $7 \times 10^{-7}$  M pyrene solution. Micellization was induced by adding 0.1 M NaOH dropwise into PDMA-*b*-PDEA solution. PDMA-*b*-PDEA micelles were stirred overnight at pH 8 and 25°C for loading of pyrene into the hydrophobic PDEA-micellar cores (Scheme 4). Of note, pyrene is a fluorescent hydrophobic molecule having very low solubility (2-3 $\mu$ M) in water. [100].



**Scheme 7.** Schematic representation of loading of Pyrene molecules into the micelle core.

The intensity of the emission peaks of pyrene change depending on the hydrophilicity of the environment [101]. The ratio of the peak centered at 375 nm to the peak centered at 393 nm ( $I_1/I_3$ ) decreases as the pyrene resides in a more hydrophobic region [89]. Thus, to assure the pyrene loading into the micellar cores, the emission spectra of pyrene before and after micellization were contrasted. Figure 22 demonstrates the emission spectra obtained from PDMA-*b*-PDEA dissolved pyrene solution at pH 3 and pH 8. As seen in the figure, the ratio of the peak centered at 375 nm to the peak centered at 393 nm decreased as the PDMA-*b*-PDEA micelles formed above critical micellization pH ( $pH > 7.5$ ), indicating the encapsulation of pyrene molecules into the PDEA micellar cores.

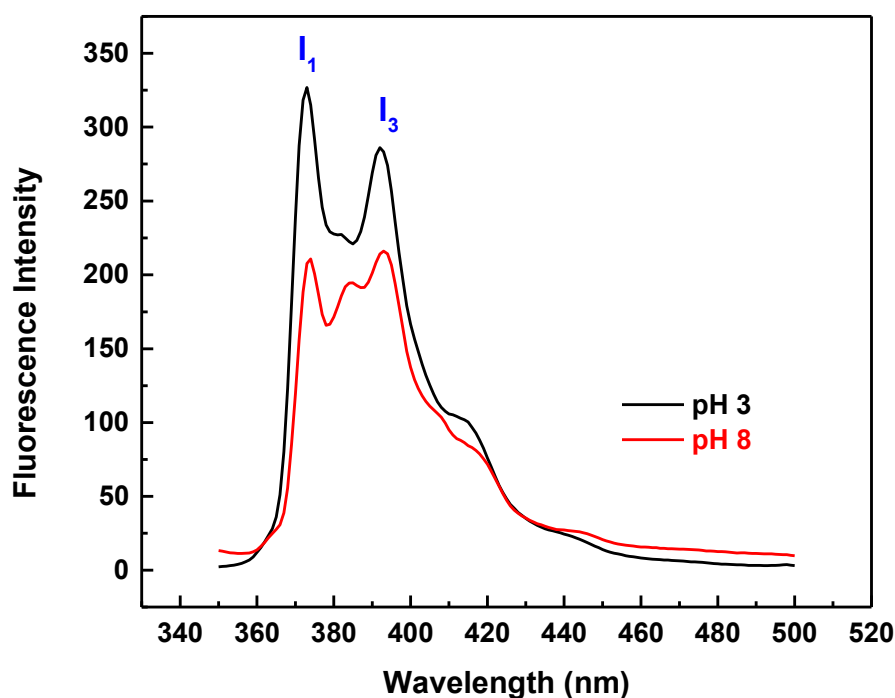
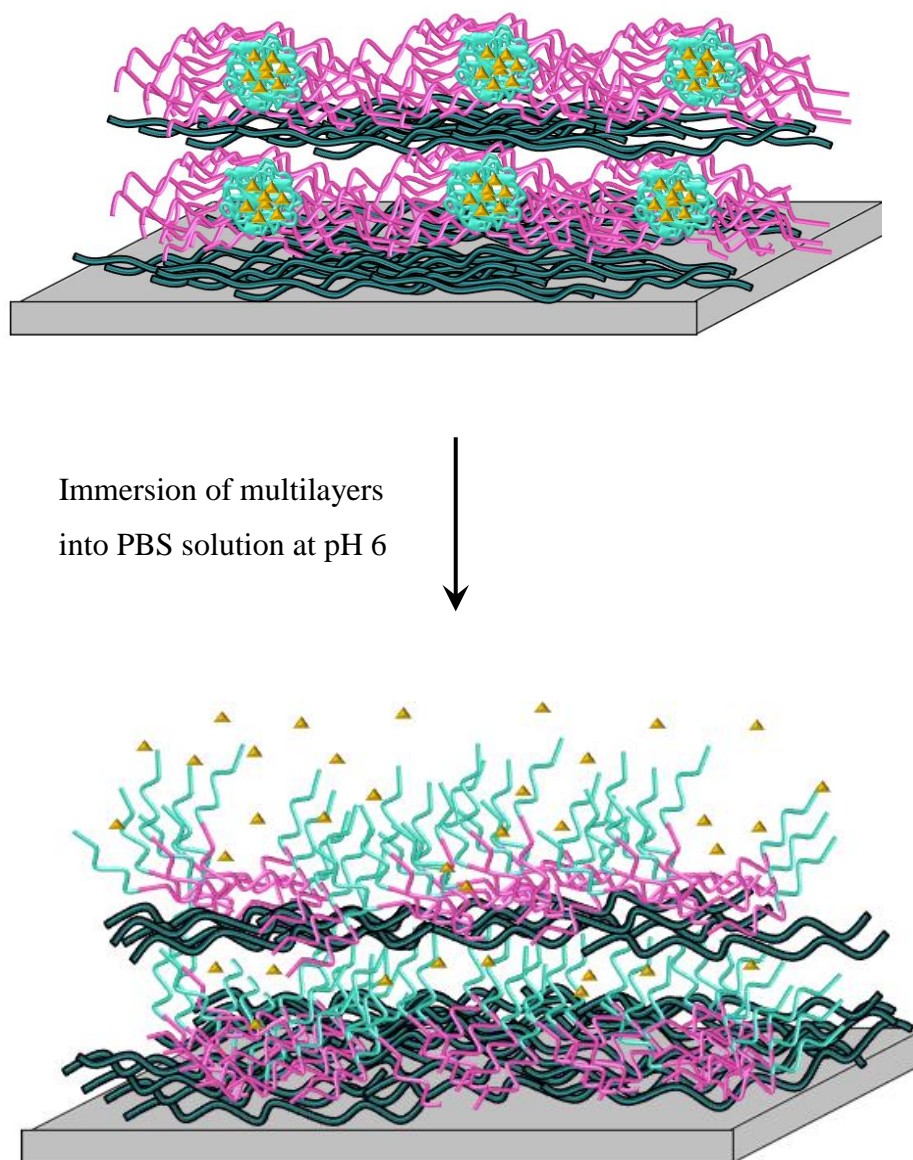


**Figure 22** Fluorescence spectra of pyrene solution in the presence of PDMA-*b*-PDEA at pH 3 and pH 8.

### 3.6.2 Pyrene Release from the Surface

Multilayers which were constructed at pH 8 and 25°C using pyrene loaded PDMA-*b*-PDEA micelles were exposed to PBS solution at pH 6 at either 25°C and 37.5°C (Scheme 8). The intensity of the peak centered at 375 nm was followed as a function of time. As a control experiment, multilayers which were constructed at pH 8 and 25°C using pyrene loaded PDMA-*b*-PDEA micelles were exposed to PBS solution at pH 8 at either 25°C and 37.5°C. The data collected at pH 6 and pH 8 were contrasted. Remember that multilayers were constructed at pH 8. As seen in Figure 23, the amount of pyrene released at pH 6 and 25°C is significantly greater than that released at pH 8 and 25°C. The greater amount of pyrene release can be correlated with the protonation of the PDEA-core blocks at pH 6 and dissolution of the micellar blocks resulting in release of pyrene from the surface. Similarly, the amount of pyrene released at pH 6 and 37.5°C was higher than that released from the surface of

the multilayers at pH 8 and 37.5°C. A comparison of the pyrene release at 25°C and 37.5°C at pH 6 showed that pyrene released in greater amount at 37.5°C. This was probably due to greater kinetic energy of the pyrene molecules at 37.5°C than that at 25°C.



**Scheme 8.** Schematic representation of disintegration of the micelles and pyrene release from the multilayers which immersed into PBS solution at pH 6.



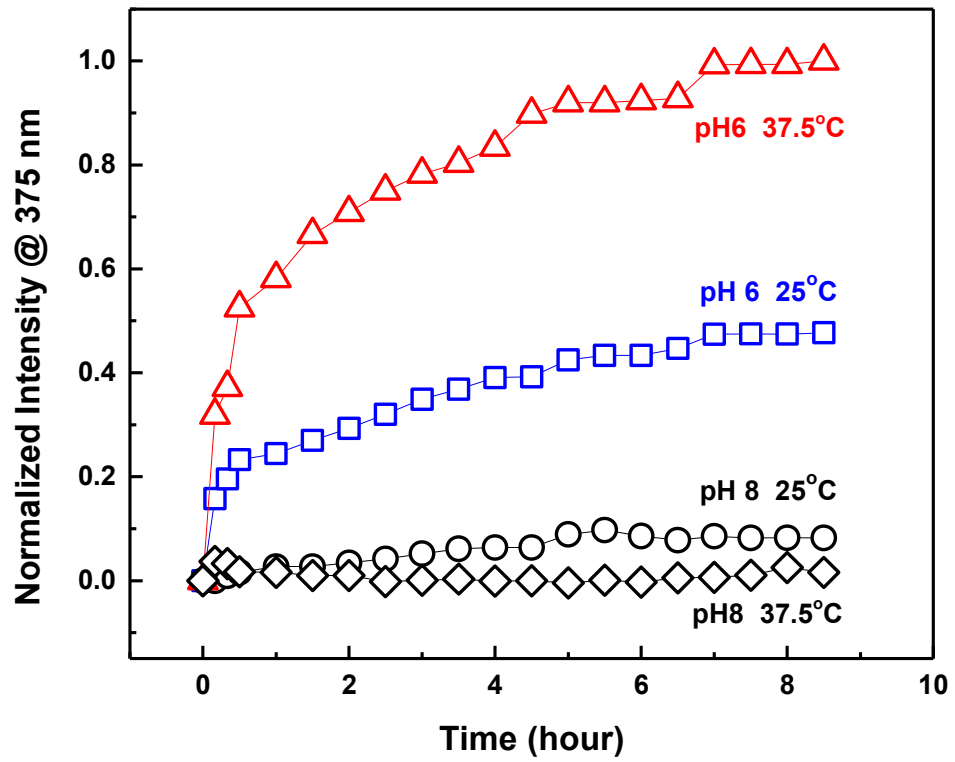


**Figure 23.** Release of pyrene from the multilayers at pH 6 at either 25°C and 37.5°C. Release at pH 8 is plotted for comparison.



## CHAPTER 4

### CONCLUSION

BCMs with pH responsive PDEA-core and pH/temperature responsive PDMA-coronae were prepared via pH-induced self-assembly of PDMA-*b*-PDEA in aqueous solution above pH 7.5. Aqueous solution properties of PDMA-*b*-PDEA micelles were examined in detail. It was found that LCST-type phase behavior of PDMA-corona was pH-dependent. The critical temperature decreased as the pH increased and the charge density on PDMA decreased.

Positively charged PDMA-*b*-PDEA micelles were then LbL deposited at the surface using negatively charged PSS at pH 8 and pH 8.5. Film deposition pH significantly affected the thickness and pH-stability of the multilayer films. Only 0.5-unit difference in pH of the polymer deposition solutions led to drastic differences in the thickness and pH-stability performance of the films at moderately acidic conditions. Multilayers were constructed at either 25°C or 30°C at pH 8 and pH 8.5. Film deposition temperature also affected the thickness and pH-stability of the multilayers. This can be explained by the LCST-type phase behavior of PDMA coronal chains and conformation transition from extended to globular conformation as the temperature approached LCST of PDMA. Importantly, temperature effect on the properties of the multilayers was pH-dependent.

In the last part of the study, pH-induced release of a hydrophobic dye, pyrene from the multilayer surface was investigated at 25°C and 37°C. Pyrene loaded PDMA-*b*-PDEA micelles were used as building blocks to construct the multilayers using PSS. Pyrene was released at moderately acidic conditions when the tertiary amino groups on PDEA-core got protonated as the pH decreased and PDMA-*b*-PDEA micelles disintegrated. It was found that increasing temperature resulted in an increase in the

amount of pyrene released from the surface at moderately acidic pH. The increase in the amount of pyrene released at 37°C was correlated with the increased diffusion rate with increasing temperature. Note that, release of biologically functional molecules at acidic conditions is desired due to acidic nature of tumor tissues or pH drop in the body at an infected site.

This thesis study presented a detailed investigation of the effect of film deposition conditions on the properties of multilayers containing dually responsive PDMA-*b*-PDEA micelles. Considering the high loading capacity of BCMs and pH as well as temperature response of multilayers, such multilayers can be promising for biomedical applications.

## REFERENCES

- [1] A. Kikuchi, T. Okano, Intelligent thermoresponsive polymeric stationary phases for aqueous chromatography of biological compounds, *Prog. Polym. Sci.* 27 (2002) 1165–1193. doi:10.1016/S0079-6700(02)00013-8.
- [2] H. Priya James, R. John, A. Alex, Smart polymers for the controlled delivery of drugs – a concise overview, *Acta Pharm. Sin. B.* 4 (2014) 120–127. doi:10.1016/j.apsb.2014.02.005.
- [3] S. Dai, P. Ravi, K.C. Tam, Thermo- and photo-responsive polymeric systems, *Soft Matter.* (2009) 2513–2533. doi:10.1039/b820044k.
- [4] B.R. Twaites, C. De Las Heras Alarcón, M. Lavigne, A. Saulnier, S.S. Pennadam, D. Cunliffe, D.C. Górecki, C. Alexander, Thermoresponsive polymers as gene delivery vectors: Cell viability, DNA transport and transfection studies, *J. Control. Release.* 108 (2005) 472–483. doi:10.1016/j.jconrel.2005.08.009.
- [5] R.A. Stile, K.E. Healy, Thermo-responsive peptide-modified hydrogels for tissue regeneration, *Biomacromolecules.* 2 (2001) 185–194. doi:10.1021/bm0000945.
- [6] A.P.N. Macromers, M.C. Hacker, L. Klouda, B.B. Ma, J.D. Kretlow, A.G. Mikos, Synthesis and Characterization of Injectable , Thermally and Chemically Synthesis and Characterization of Injectable , Thermally and Chemically Gelable , Amphiphilic Poly ( N-isopropylacrylamide ) -Based Macromers, *Society.* (2008) 1558–1570. doi:10.1021/bm8000414.
- [7] K.B. Doorty, T.A. Golubeva, A. V. Gorelov, Y.A. Rochev, L.T. Allen, K.A. Dawson, W.M. Gallagher, A.K. Keenan, Poly(N-isopropylacrylamide) copolymer films as potential vehicles for delivery of an antimetabolic agent to

- vascular smooth muscle cells, *Cardiovasc. Pathol.* 12 (2003) 105–110. doi:10.1016/S1054-8807(02)00165-5.
- [8] G. Molinaro, J.C. Leroux, J. Damas, A. Adam, Biocompatibility of thermosensitive chitosan-based hydrogels: An in vivo experimental approach to injectable biomaterials, *Biomaterials.* 23 (2002) 2717–2722. doi:10.1016/S0142-9612(02)00004-2.
- [9] Y. Qiu, K. Park, Environment-sensitive hydrogels for drug delivery, *Adv. Drug Deliv. Rev.* 64 (2012) 49–60. doi:10.1016/j.addr.2012.09.024.
- [10] J. Seuring, S. Agarwal, Polymers with upper critical solution temperature in aqueous solution, *Macromol. Rapid Commun.* 33 (2012) 1898–1920. doi:10.1002/marc.201200433.
- [11] S. Singh, D.C. Webster, J. Singh, Thermosensitive polymers: Synthesis, characterization, and delivery of proteins, *Int. J. Pharm.* 341 (2007) 68–77. doi:10.1016/j.ijpharm.2007.03.054.
- [12] C. Weber, R. Hoogenboom, U.S. Schubert, Temperature responsive biocompatible polymers based on poly(ethylene oxide) and poly(2-oxazoline)s, *Prog. Polym. Sci.* 37 (2012) 686–714. doi:10.1016/j.progpolymsci.2011.10.002.
- [13] M.I. Gibson, R.K. O'Reilly, To aggregate, or not to aggregate? considerations in the design and application of polymeric thermally-responsive nanoparticles, *Chem. Soc. Rev.* 42 (2013) 7204–7213. doi:10.1039/C3CS60035A.
- [14] Y. Okada, F. Tanaka, Cooperative hydration, chain collapse, and flat LCST behavior in aqueous poly(N-isopropylacrylamide) solutions, *Macromolecules.* 38 (2005) 4465–4471. doi:10.1021/ma0502497.
- [15] C. Boutris, E.G. Chatzi, C. Kiparissides, Characterization of the LCST behaviour of aqueous poly(N-isopropylacrylamide) solutions by thermal and cloud point techniques, *Polymer (Guildf).* 38 (1997) 2567–2570.

doi:10.1016/S0032-3861(97)01024-0.

- [16] D.J. Phillips, M.I. Gibson, Towards being genuinely smart: “isothermally-responsive” polymers as versatile, programmable scaffolds for biologically-adaptable materials, *Polym. Chem.* 6 (2015) 1033–1043. doi:10.1039/C4PY01539H.
- [17] G. Kocak, C. Tuncer, V. Bütün, pH-Responsive polymers, *Polym. Chem.* 8 (2017) 144–176. doi:10.1039/C6PY01872F.
- [18] A. Chan, R.P. Orme, R.A. Fricker, P. Roach, Remote and local control of stimuli responsive materials for therapeutic applications, *Adv. Drug Deliv. Rev.* 65 (2013) 497–514. doi:10.1016/j.addr.2012.07.007.
- [19] C.-L. Peng, L.-Y. Yang, T.-Y. Luo, P.-S. Lai, S.-J. Yang, W.-J. Lin, M.-J. Shieh, Development of pH sensitive 2-(diisopropylamino)ethyl methacrylate based nanoparticles for photodynamic therapy., *Nanotechnology.* 21 (2010) 155103. doi:10.1088/0957-4484/21/15/155103.
- [20] A.C. Foss, T. Goto, M. Morishita, N.A. Peppas, Development of acrylic-based copolymers for oral insulin delivery, *Eur. J. Pharm. Biopharm.* 57 (2004) 163–169. doi:10.1016/S0939-6411(03)00145-0.
- [21] X. Jin, Y. Lo Hsieh, PH-responsive swelling behavior of poly(vinyl alcohol)/poly(acrylic acid) bi-component fibrous hydrogel membranes, *Polymer (Guildf).* 46 (2005) 5149–5160. doi:10.1016/j.polymer.2005.04.066.
- [22] J.E. Elliott, M. MacDonald, J. Nie, C.N. Bowman, Structure and swelling of poly(acrylic acid) hydrogels: Effect of pH, ionic strength, and dilution on the crosslinked polymer structure, *Polymer (Guildf).* 45 (2004) 1503–1510. doi:10.1016/j.polymer.2003.12.040.
- [23] V. Bütün, S.P. Armes, N.C. Billingham, Synthesis and aqueous solution properties of near-monodisperse tertiary amine methacrylate homopolymers and diblock copolymers, *Polymer (Guildf).* 42 (2001) 5993–6008.

doi:10.1016/S0032-3861(01)00066-0.

- [24] R. Langer, D.A. Tirrell, Designing materials for biology and medicine, *Nature*. 428 (2004) 487–492. doi:10.1038/nature02388.
- [25] J.S. Ross, D.P. Schenkein, R. Pietrusko, M. Rolfe, G.P. Linette, J. Stec, N.E. Stagliano, G.S. Ginsburg, W.F. Symmans, L. Pusztai, G.N. Hortobagyi, Targeted therapies for cancer 2004, *Am J Clin Pathol*. 122 (2004) 598–609. doi:10.1309/5CWP-U41A-FR1V-YM3F.
- [26] K. Kataoka, A. Harada, Y. Nagasaki, Block copolymer micelles for drug delivery: Design, characterization and biological significance, *Adv. Drug Deliv. Rev.* 47 (2001) 113–131. doi:10.1016/S0169-409X(00)00124-1.
- [27] P. Grodzinski, Cancer Nanotechnology – Opportunities and Challenges – View from the NCI Alliance for Nanotechnology in Cancer, *Natl. Cancer Inst.* (2011) 1–15.
- [28] Z. Ge, S. Liu, Functional block copolymer assemblies responsive to tumor and intracellular microenvironments for site-specific drug delivery and enhanced imaging performance., *Chem. Soc. Rev.* 42 (2013) 7289–325. doi:10.1039/c3cs60048c.
- [29] J. Hu, G. Zhang, S. Liu, Enzyme-responsive polymeric assemblies, nanoparticles and hydrogels, *Chem. Soc. Rev.* 41 (2012) 5933. doi:10.1039/c2cs35103j.
- [30] F. Ercole, T.P. Davis, R. a. Evans, Photo-responsive systems and biomaterials: photochromic polymers, light-triggered self-assembly, surface modification, fluorescence modulation and beyond, *Polym. Chem.* 1 (2010) 37. doi:10.1039/b9py00300b.
- [31] J. Hu, S. Liu, Engineering responsive polymer building blocks with host-guest molecular recognition for functional applications, *Acc. Chem. Res.* 47 (2014) 2084–2095. doi:10.1021/ar5001007.



- [32] X. Hu, S. Liu, Recent advances towards the fabrication and biomedical applications of responsive polymeric assemblies and nanoparticle hybrid superstructures, *Dalt. Trans.* 44 (2015) 3904–3922. doi:10.1039/C4DT03609C.
- [33] J. Yin, Y. Chen, Z.H. Zhang, X. Han, Stimuli-responsive block copolymer-based assemblies for cargo delivery and theranostic applications, *Polymers (Basel)*. 8 (2016). doi:10.3390/polym8070268.
- [34] S. Liu, R. Maheshwari, K.L. Kiick, Polymer-based therapeutics, *Macromolecules*. 42 (2009) 3–13. doi:10.1021/ma801782q.
- [35] C.-M.J. Hu, R.H. Fang, B.T. Luk, L. Zhang, Polymeric nanotherapeutics: clinical development and advances in stealth functionalization strategies., *Nanoscale*. 6 (2014) 65–75. doi:10.1039/c3nr05444f.
- [36] Z. Liu, Z. Niu, Temperature responsive 3D structure of rod-like bionanoparticles induced by depletion interaction, *Chinese J. Polym. Sci.* 32 (2014) 1271–1275. doi:10.1007/s10118-014-1523-9.
- [37] R.D. Issels, Hyperthermia adds to chemotherapy, *Eur. J. Cancer*. 44 (2008) 2546–2554. doi:10.1016/j.ejca.2008.07.038.
- [38] M. Moffitt, K. Khougaz, a Eisenberg, Micellization of ionic block copolymers, *Acc. Chem. Res.* 29 (1996) 95–102. doi:10.1021/AR940080.
- [39] H.G. Zachmann, *Advances in Polymer Science*, 1976. doi:10.1524/zpch.1976.99.4-6.310.
- [40] M. Lazzari, G. Liu, S. Lecommandoux, *Block copolymers in nanscience*, 2006.
- [41] L. Franck-Lacaze, P. Sifat, P. Huguet, Determination of the pKa of poly (4-vinylpyridine)-based weak anion exchange membranes for the investigation of the side proton leakage, *J. Memb. Sci.* 326 (2009) 650–658.

doi:10.1016/j.memsci.2008.10.054.

- [42] A. Thomas J. Martin, K. Prochazka, P. Munk, S. E. Webber, pH-Dependent Micellization of Poly(2-vinylpyridine)-block-poly(ethylene oxide), *Macromolecules*. 29 (1996) 6071–6073. doi:10.1177/004051758105100910.
- [43] S.K. Varshney, R. Je, Water-Soluble Complexes Formed by Poly ( 2-vinylpyridinium ) - block -poly ( ethylene oxide ) and Poly ( sodium methacrylate ) - block -poly ( ethylene oxide ) Copolymers, (2001) 3361–3366.
- [44] Y.L. Luo, R.J. Huang, F. Xu, Y.S. Chen, PH-Sensitive biodegradable PMAA2-b-PLA-b-PMAA2 H-type multiblock copolymer micelles: Synthesis, characterization, and drug release applications, *J. Mater. Sci.* 49 (2014) 7730–7741. doi:10.1007/s10853-014-8483-x.
- [45] L.I. Gabaston, S.A. Furlong, R.A. Jackson, S.P. Armes, Direct synthesis of novel acidic and zwitterionic block copolymers via TEMPO-mediated living free-radical polymerization, *Polymer (Guildf)*. 40 (1999) 4505–4514. doi:10.1016/S0032-3861(98)00689-2.
- [46] L. Bailey, M. Vamvakaki, N.C. Billingham, S.P. Armes, Synthesis and Aqueous Solution Properties of Novel Hydrophilic/Hydrophilic Block Copolymers based on Tertiary Amine Methacrylates and Poly (Ethylene Oxide), *Chem. Commun.* (1997) 671–672. doi:10.1039/A700772H.
- [47] X. André, M. Zhang, A.H.E. Müller, Thermo- and pH-responsive micelles of poly(acrylic acid)-block-poly(N,N- diethylacrylamide), *Macromol. Rapid Commun.* 26 (2005) 558–563. doi:10.1002/marc.200400510.
- [48] H. Wei, X.Z. Zhang, Y. Zhou, S.X. Cheng, R.X. Zhuo, Self-assembled thermoresponsive micelles of poly(N-isopropylacrylamide-b- methyl methacrylate), *Biomaterials*. 27 (2006) 2028–2034. doi:10.1016/j.biomaterials.2005.09.028.

- [49] B. Meets, *Biotechnology Meets Materials Science*, *Mater. Sci.* 40 (2001) 4128–4158. doi:10.1002/1521-3773(20011119)40:22<4128::aid-anie4128>3.0.co;2-s.
- [50] Z. Matharu, A.J. Bhandodkar, V. Gupta, B.D. Malhotra, *Fundamentals and application of ordered molecular assemblies to affinity biosensing.*, *Chem. Soc. Rev.* 41 (2012) 1363–1402. doi:10.1039/c1cs15145b.
- [51] K. Ariga, X. Hu, S. Mandal, J.P. Hill, *By what means should nanoscaled materials be constructed: molecule, medium, or human?*, *Nanoscale.* 2 (2010) 198–214. doi:10.1039/b9nr00105k.
- [52] K. Tang, N.A.M. Besseling, *Formation of polyelectrolyte multilayers: ionic strengths and growth regimes.*, *Soft Matter.* 12 (2016) 1032–40. doi:10.1039/c5sm02118a.
- [53] S.T. Dubas, J.B. Schlenoff, *by Salt*, (2001) 7725–7727.
- [54] G. Decher, *Fuzzy Nanoassemblies: Toward Layered Polymeric Multicomposites*, *Science* (80-. ). 277 (1997) 1232–1237. doi:10.1126/science.277.5330.1232.
- [55] W.B. Stockton, M.F. Rubner, *Molecular-Level Processing of Conjugated Polymers. 4. Layer-by-Layer Manipulation of Polyaniline via Hydrogen-Bonding Interactions*, *Macromolecules.* 30 (1997) 2717–2725. doi:10.1021/ma9700486.
- [56] L. Wang, Z. Wang, X. Zhang, J. Shen, L. Chi, H. Fuchs, *A new approach for the fabrication of an alternating multilayer film of poly(4-vinylpyridine) and poly(acrylic acid) based on hydrogen bonding*, *Macromol. Rapid Commun.* 18 (1997) 509–514. doi:10.1002/marc.1997.030180609.
- [57] S. Leininger, B. Olenyuk, P.J. Stang, *Self-Assembly of Discrete Cyclic Nanostructures Mediated by Transition Metals*, *Chem. Rev.* 100 (2000) 853–907. doi:doi:10.1021/cr9601324.

- [58] Y. Shimazaki, M. Mitsuishi, S. Ito, M. Yamamoto, Preparation of the Layer-by-Layer Deposited Ultrathin Film Based on the Charge-Transfer Interaction, *Langmuir*. 13 (1997) 1385–1387. doi:10.1021/la9609579.
- [59] H. Xiong, Z. Zhou, Z. Wang, X. Zhang, J. Shen, New approach to fabrication of a self-organizing film of heterostructured polymer/CdS nanoparticles, *Supramol. Sci.* 5 (1998) 623–626. doi:10.1016/S0968-5677(98)00089-3.
- [60] A.K. Lvov, Y. Ichinose, I. Kunitake, T. Layer-by-layer Architectures of Concanavalin, *J. Chem. Soc., Chem. Commun.* (1995) 2313–2314.
- [61] R. Article, D. Rawtani, Y.K. Agrawal, Emerging Strategies and Applications of Review Article, (2014) 1–15.
- [62] P. Koegler, A. Clayton, H. Thissen, G.N.C. Santos, P. Kingshott, The influence of nanostructured materials on biointerfacial interactions, *Adv. Drug Deliv. Rev.* 64 (2012) 1820–1839. doi:10.1016/j.addr.2012.06.001.
- [63] D.G. Castner, B.D. Ratner, *Biomedical surface science: Foundations to frontiers*, 2002. doi:10.1016/S0039-6028(01)01587-4.
- [64] M. Assemblies, G. Mole-, R. Lbl, A. Mechanism, G.M. Assemblies, F. Polymeric, U. Lbl, Assemblies et al. - 2014 - Molecular Interactions Driving the Layer-by-Layer Assembly of Multilayers Joa o.pdf, (2014). doi:10.1021/cr400531v.
- [65] C. Djugnat, G.B. Sukhorukov, pH-responsive properties of hollow polyelectrolyte microcapsules templated on various cores, *Langmuir*. 20 (2004) 7265–7269. doi:10.1021/la049706n.
- [66] A.J. Chung, M.F. Rubner, Methods of loading and releasing low molecular weight cationic molecules in weak polyelectrolyte multilayer films, *Langmuir*. 18 (2002) 1176–1183. doi:10.1021/la010873m.
- [67] K. Yoshida, K. Sato, J. Anzai, Layer-by-layer polyelectrolyte films containing

- insulin for pH-triggered release, *J. Mater. Chem.* 20 (2010) 1546–1552. doi:10.1039/B918226H.
- [68] E. Kharlampieva, S.A. Sukhishvili, Release of a dye from hydrogen-bonded and electrostatically assembled polymer films triggered by adsorption of a polyelectrolyte, *Langmuir*. 20 (2004) 9677–9685. doi:10.1021/la048763d.
- [69] I. Erel, H.E. Karahan, C. Tuncer, V. Bütün, a. L. Demirel, Hydrogen-bonded multilayers of micelles of a dually responsive dicationic block copolymer, *Soft Matter*. 8 (2012) 827. doi:10.1039/c1sm06248d.
- [70] J.F. Quinn, F. Caruso, Facile Tailoring of Film Morphology and Release Properties Using Layer-by-Layer Assembly of Thermoresponsive Materials, *Langmuir*. 20 (2004) 20–22. doi:10.1021/la0360310.
- [71] K. Glinel, C. Déjugnat, M. Prevot, B. Schöler, M. Schönhoff, R. v. Klitzing, Responsive polyelectrolyte multilayers, *Colloids Surfaces A Physicochem. Eng. Asp.* 303 (2007) 3–13. doi:10.1016/j.colsurfa.2007.02.052.
- [72] Z. Zhu, N. Gao, H. Wang, S.A. Sukhishvili, Temperature-triggered on-demand drug release enabled by hydrogen-bonded multilayers of block copolymer micelles, *J. Control. Release*. 171 (2013) 73–80. doi:10.1016/j.jconrel.2013.06.031.
- [73] L. Xu, Z. Zhu, S.A. Sukhishvili, Polyelectrolyte multilayers of diblock copolymer micelles with temperature-responsive cores, *Langmuir*. 27 (2011) 409–415. doi:10.1021/la1038014.
- [74] R. Konradi, C. Acikgoz, M. Textor, Polyoxazolines for nonfouling surface coatings - A direct comparison to the gold standard PEG, *Macromol. Rapid Commun.* 33 (2012) 1663–1676. doi:10.1002/marc.201200422.
- [75] I. Erel, H. Schlaad, A.L. Demirel, Effect of structural isomerism and polymer end group on the pH-stability of hydrogen-bonded multilayers, *J. Colloid Interface Sci.* 361 (2011) 477–482. doi:10.1016/j.jcis.2011.05.033.

- [76] A. Antunes, M. Dierendonck, G. Vancoillie, J.P. Remon, R. Hoogenboom, B.G. De Geest, Hydrogen bonded polymeric multilayer films assembled below and above the cloud point temperature, *Chem. Commun.* 49 (2013) 9663–9665. doi:10.1039/c3cc45068f.
- [77] A. Sundaramurthy, M. Vergaelen, S. Maji, R. Auzély-Velty, Z. Zhang, B.G. De Geest, R. Hoogenboom, Hydrogen Bonded Multilayer Films Based on Poly(2-oxazoline)s and Tannic Acid, *Adv. Healthc. Mater.* 3 (2014) 2040–2047. doi:10.1002/adhm.201400377.
- [78] A. Osypova, D. Magnin, P. Sibret, A. Aqil, C. Jérôme, C. Dupont-Gillain, C.-M. Pradier, S. Demoustier-Champagne, J. Landoulsi, Dual stimuli-responsive coating designed through layer-by-layer assembly of PAA-b-PNIPAM block copolymers for the control of protein adsorption, *Soft Matter*. 11 (2015) 8154–8164. doi:10.1039/C5SM01545F.
- [79] P. Yusan, I. Tuncel, V. Butun, A.L. Demirel, I. Erel-Goktepe, pH-responsive layer-by-layer films of zwitterionic block copolymer micelles, *Polym. Chem.* 5 (2014) 3777–3787. doi:10.1039/c4py00040d.
- [80] H. Arslan, O. Zirtil, V. Bütün, The synthesis and solution behaviors of novel amphiphilic block copolymers based on d-galactopyranose and 2-(dimethylamino)ethyl methacrylate, *Eur. Polym. J.* 49 (2013) 4118–4129. doi:10.1016/j.eurpolymj.2013.09.018.
- [81] V. Bütün, Selective betainization of 2-(dimethylamino)ethyl methacrylate residues in tertiary amine methacrylate diblock copolymers and their aqueous solution properties, *Polymer (Guildf)*. 44 (2003) 7321–7334. doi:10.1016/j.polymer.2003.09.027.
- [82] V. Bütün, S.P. Armes, N.C. Billingham, Selective quaternization of 2-(dimethylamino)ethyl methacrylate residues in tertiary amine methacrylate diblock copolymers, *Macromolecules*. 34 (2001) 1148–1159. doi:10.1021/ma001550k.

- [83] A.S. Lee, A.P. Gast, V. Bütün, S.P. Armes, Characterizing the structure of pH dependent polyelectrolyte block copolymer micelles, *Macromolecules*. 32 (1999) 4302–4310. doi:10.1021/ma981865o.
- [84] K. Sakai, E.G. Smith, G.B. Webber, E.J. Wanless, V. Bütün, Effects of copolymer concentration and chain length on the pH-responsive behavior of diblock copolymer micellar films, 303 (2006) 372–379. doi:10.1016/j.jcis.2006.07.077.
- [85] K. Sakai, E.G. Smith, G.B. Webber, C. Schatz, E.J. Wanless, V. Bütün, S.P. Armes, S. Biggs, pH-responsive diblock copolymer micelles at the silica/aqueous solution interface: Adsorption kinetics and equilibrium studies., *J. Phys. Chem. B*. 110 (2006) 14744–14753. doi:10.1021/jp062830q.
- [86] T. Addison, O.J. Cayre, S. Biggs, S.P. Armes, D. York, Multi-layer films of block copolymer micelles adsorbed to colloidal templates., *Philos. Trans. A. Math. Phys. Eng. Sci.* 368 (2010) 4293–4311. doi:10.1098/rsta.2010.0151.
- [87] S. Biggs, K. Sakai, T. Addison, A. Schmid, S.P. Armes, M. Vamvakaki, V. Bütün, G. Webber, Layer-by-layer formation of smart particle coatings using oppositely charged block copolymer micelles, *Adv. Mater.* 19 (2007) 247–250. doi:10.1002/adma.200601553.
- [88] T. Addison, O.J. Cayre, S. Biggs, S.P. Armes, D. York, Incorporation of Block Copolymer Micelles into Multilayer Films for Use as Nanodelivery Systems Addison, T., Cayre, O. J., Biggs, S., Armes, S. P., & York, D. (2008). Incorporation of Block Copolymer Micelles into Multilayer Films for Use as Nanodelivery S, 19 (2008) 13328–13333.
- [89] C. Schatz, E.G. Smith, S.P. Armes, E.J. Wanless, Reversible pH-triggered encapsulation and release of pyrene by adsorbed block copolymer micelles, *Langmuir*. 24 (2008) 8325–8331. doi:10.1021/la801127r.
- [90] J. Xu, S. Luo, W. Shi, S. Liu, Two-stage collapse of unimolecular micelles with double thermoresponsive coronas, *Langmuir*. 22 (2006) 989–997.

doi:10.1021/la0522707.

- [91] F. a. Plamper, M. Ruppel, A. Schmalz, O. Borisov, M. Ballauff, A.H.E. Müller, Tuning the Thermoresponsive Properties of Weak Polyelectrolytes: Aqueous Solutions of Star-Shaped and Linear Poly( N,N -dimethylaminoethyl Methacrylate), *Macromolecules*. 40 (2007) 8361–8366. doi:10.1021/ma071203b.
- [92] M. Thomas, M. Gajda, C. Amiri Naini, S. Franzka, M. Ulbricht, N. Hartmann, Poly(N,N-dimethylaminoethyl methacrylate) Brushes: PH-Dependent Switching Kinetics of a Surface-Grafted Thermoresponsive Polyelectrolyte, *Langmuir*. 31 (2015) 13426–13432. doi:10.1021/acs.langmuir.5b03448.
- [93] M.D. Kurkuri, M.R. Nussio, A. Deslandes, N.H. Voelcker, Thermosensitive copolymer coatings with enhanced wettability switching, *Langmuir*. 24 (2008) 4238–4244. doi:10.1021/la703668s.
- [94] D. Fournier, R. Hoogenboom, H.M.L. Thijs, R.M. Paulus, U.S. Schubert, D. Fournier, R. Hoogenboom, H.M.L. Thijs, R.M. Paulus, U.S. Schubert, Tunable pH- and Temperature-Sensitive Copolymer Libraries by Reversible Addition – Fragmentation Chain Transfer Copolymerizations of Methacrylates Tunable pH- and Temperature-Sensitive Copolymer Libraries by Reversible Addition - Fragmentation Chain Trans, (2007) 915–920. doi:10.1021/ma062199r.
- [95] S.H. Yuk, S.H. Cho, S.H. Lee, pH/Temperature-Responsive Polymer Composed of Poly((N,N-dimethylamino)ethyl methacrylate-co-ethylacrylamide), *Macromolecules*. 9297 (1997) 6856–6859.
- [96] C. Salvi, X. Lyu, A.M. Peterson, Effect of Assembly pH on Polyelectrolyte Multilayer Surface Properties and BMP-2 Release, *Biomacromolecules*. 17 (2016) 1949–1958. doi:10.1021/acs.biomac.5b01730.
- [97] J. Fu, J. Ji, L. Shen, A. Ku, A. Rosenhahn, J. Shen, M. Grunze, pH-Amplified Exponential Growth Multilayers : A Facile Method to Develop Hierarchical



Micro- and Nanostructured Surfaces pH-Amplified Exponential Growth Multilayers: A Facile Method to Develop Hierarchical Micro- and Nanostructured Surfaces, *Society*. 25 (2009) 672–675. doi:10.1021/la803692v.

- [98] Z. Sui, J.B. Schlenoff, Phase separations in pH-responsive polyelectrolyte multilayers: Charge extrusion versus charge expulsion, *Langmuir*. 20 (2004) 6026–6031. doi:10.1021/la0495985.
- [99] T. Mauser, C. Déjugnat, H. Möhwald, G.B. Sukhorukov, Microcapsules made of weak polyelectrolytes: Templating and stimuli-responsive properties, *Langmuir*. 22 (2006) 5888–5893. doi:10.1021/la060088f.
- [100] K. kalyanasundara. J.K.thomas, Environmental effects on vibronic band intensities in pyrene monomer fluorescence and their application in studies of micellar systems, *J. Am. Chem. Soc.* 2039 (1977) 2039–2044. doi:10.1021/ja00449a004.
- [101] M. Hans, K. Shimoni, D. Danino, S.J. Siégel, A. Lowman, Synthesis and characterization of mPEG-PLA prodrug micelles, *Biomacromolecules*. 6 (2005) 2708–2717. doi:10.1021/bm050188k.